nature communications

Article

https://doi.org/10.1038/s41467-024-53242-0

A single-dose circular RNA vaccine prevents Zika virus infection without enhancing dengue severity in mice

Received: 7 March 2024

Accepted: 7 October 2024

Published online: 16 October 2024

Check for updates

Xinglong Liu[1,2,9], Zhengfeng Li[1,9], Xiaoxia Li[1,2,9], Weixuan Wu[1,2], Huadong Jiang[1,3], Yufen Zheng[1,2], Junjie Zhou[1], Xianmiao Ye[4], Junnan Lu[1], Wei Wang[5], Lei Yu[6], Yiping Li[7], Linbing Qu[1], Jianhua Wang[1], Feng Li[6], Ling Chen[1,8] ✉, Linping Wu[1,2] ✉ & Liqiang Feng[1,2] ✉

Antibody-dependent enhancement (ADE) is a potential concern for the development of Zika virus (ZIKV) vaccines. Cross-reactive but poorly neutralizing antibodies, usually targeting viral pre-membrane or envelope (E) proteins, can potentially enhance dengue virus (DENV) infection. Although E domain III (EDIII) contains ZIKV-specific epitopes, its immunogenicity is poor. Here, we show that dimeric EDIII, fused to human IgG1 Fc fragment (EDIII-Fc) and encoded by circular RNA (circRNA), induces better germinal center reactions and higher neutralizing antibodies compared to circRNAs encoding monomeric or trimeric EDIII. Two doses of circRNAs encoding EDIII-Fc and ZIKV nonstructural protein NS1, another protective antigen, prevent lethal ZIKV infection in neonates born to immunized C57BL/6 mice and in interferon-α/β receptor knockout adult C57BL/6 mice. Importantly, a single-dose optimized circRNA vaccine with improved antigen expression confers potent and durable protection without inducing obvious DENV ADE in mice, laying the groundwork for developing flavivirus vaccines based on circRNAs encoding EDIII-Fc and NS1.

Zika virus (ZIKV), a mosquito-borne flavivirus within the family *Flaviviridae*, is phylogenetically close to dengue virus (DENV), which includes four distinct serotypes. Historically, ZIKV infection sporadically led to mild, self-limited dengue-like illnesses[1]. Since 2007, large ZIKV outbreaks have emerged across Africa, the Americas, Asia and the Pacific, affecting up to 92 countries or territories with reported evidence of mosquito-transmitted ZIKV infection[2]. During recent epidemics, ZIKV infection has been linked to severe neurological disorders, including Guillain-Barré syndrome in adults and microcephaly in newborns[1]. Despite a decline in ZIKV transmission since 2017, several countries continue to report infection clusters[3]. The *Aedes aegypti* mosquito, a shared vector for ZIKV and DENV, has extended its habitat from tropical and subtropical regions to temperate regions, increasing the risk of future epidemics[4]. Currently, there are still no ZIKV vaccines approved for clinical use.

An important safety concern for vaccine development against ZIKV is the antibody-dependent enhancement (ADE) of infection between ZIKV and DENV. It has been recognized that pre-existing

[1]State Key Laboratory of Respiratory Disease, CAS Key Laboratory of Regenerative Biology, Guangzhou Institutes of Biomedicine and Health, Chinese Academy of Sciences, Guangzhou 510530, China. [2]University of Chinese Academy of Sciences, Beijing 100049, China. [3]School of Life Science, University of Science and Technology of China, Hefei 230026, China. [4]School of Public Health (Shenzhen), Sun Yat-sen University, Shenzhen 518107, China. [5]Bioland Laboratory, Guangzhou 510005, China. [6]Guangzhou Eighth People's Hospital, Guangzhou Medical University, Guangzhou 510440, China. [7]Institute of Human Virology, Zhongshan School of Medicine, Sun Yat-sen University, Guangzhou 501180, China. [8]Guangzhou National Laboratory, Guangzhou 510005, China. [9]These authors contributed equally: Xinglong Liu, Zhengfeng Li, Xiaoxia Li. ✉e-mail: chen_ling@gibh.ac.cn; wu_linping@gibh.ac.cn; feng_liqiang@gibh.ac.cn

immunity to ZIKV aggravates subsequent DENV infection in both animal models and humans[5,6]. The conserved epitopes on ZIKV premembrane (prM) and envelope (E) proteins are prone to eliciting non- or sub-neutralizing, yet cross-reactive antibodies that facilitate DENV entry through Fcγ receptors (FcγRs), thereby worsening infection and disease[6,7]. These concerns necessitate the caution with vaccine candidates that rely on full-length E protein or its combination with prM. Masking or modifying these epitopes on the E protein, especially those in the fusion loop of domain II (EDII) and potentially those in domain I (EDI), reduces, but is difficult to completely eliminate, ADE-prone antibodies[8–11]. The domain III (EDIII) of the E protein is preferable because it mediates viral binding to cellular receptors and exhibits less similarity among flaviviruses compared to EDI and EDII[12]. EDIII-targeting antibodies are usually type-specific and have high neutralizing potency[7,12,13]. Nonetheless, the immunogenicity of EDIII is inherently poor[7], which may necessitate multiple doses to achieve adequate protective immunity[14,15].

The nonstructural protein NS1 of ZIKV is attractive as another protective antigen[16,17]. Membrane-bound NS1 serves as the scaffold for the assembly of viral replication complex in endoplasmic reticulum and inhibits complement activation on cell surfaces[16]. Secreted NS1 increases the permeability of umbilical vein and brain endothelial cells, contributing to vascular leakage in the placentas and brains[16,18]. Interestingly, anti-NS1 antibodies can mitigate these harmful effects[16,19–21]. Anti-NS1 antibodies also mediate effector functions to facilitate viral clearance[20–23]. NS1-based vaccines have shown protective effects in several animal models[24–27]. Importantly, anti-NS1 antibodies do not cause ADE, because NS1 proteins are absent from viral particles[16]. Therefore, it is reasonable to combine EDIII and NS1 to maximize the protective immunity.

An ideal ZIKV vaccine would confer effective protection through a single-dose inoculation, thereby shortening the period of risk and improving vaccine acceptance. Such a vaccine requires robust genetic vectors that efficiently express and present antigens to host immunity. Circular RNA (circRNA) has emerged as a noteworthy candidate. Being single-stranded and covalently closed, circRNAs are naturally resistant to degradation by exonuclease, resulting in better in vitro and in vivo stability compared to linear RNA molecules[28,29]. Consequently, circRNAs may be a viable option for ZIKV immunization in endemic regions lacking cold chain facilities[28,29]. Furthermore, circRNAs may confer prolonged antigen expression over linear mRNAs in vivo, potentially leading to durable protective immunity[28,29]. It has been reported that circRNA vaccines elicit neutralizing antibody (nAb) responses and Th1-skewed T cell responses of higher quality than those elicited by linear mRNA vaccines[30].

Here, we report a circRNA-based ZIKV vaccine strategy. We fused EDIII to human IgG1 Fc region, a known method for extending antigen half-life through neonatal Fc receptor (FcRn) recycling mechanisms and for increasing the avidity for B-cell receptors through antigen dimerization[31,32]. Additionally, this fusion potentially enhances antigen uptake and presentation by FcγR-expressing antigen presenting cells in draining lymph nodes[33,34], thereby improving the immunogenicity. We evaluated the protective efficacy of EDIII-Fc and NS1 circRNAs in the neonates born to immunized mice and in adult mice lacking the interferon-α/β receptor (*Ifnar*$^{-/-}$). We also assessed the risks of ADE associated with passive immune sera transfer or active immunization. Our results demonstrate that, following optimization, a single-dose administration of circRNA vaccine effectively prevents ZIKV infection without causing significant ADE of DENV infection in mice.

Results

EDIII-Fc circRNA has better immunogenicity than EDIII-Fd or EDIII circRNA

We designed three types of circRNAs, each encoding a different version of EDIII: a monomeric form (EDIII, residues 298 to 409 of ZIKV E protein), a dimeric EDIII-Fc fusion, and a trimeric EDIII fused to the foldon domain of bacteriophage T4 fibritin (EDIII-Fd), the latter being a motif commonly used to initiate trimerization[35]. The synthesis of circRNAs involved a permuted intron-exon (PIE) splicing strategy, employing a group I catalytic intron derived from Anabaena pre-tRNA (Ana). This strategy showed circularization efficiency exceeding 95%[36]. The two flanking transposed halves of split intron auto-catalytically excise, and the two flanking exons ligate in tandem transesterification reactions (Fig. 1a). We inserted the fragments covering the internal ribosome entry site (IRES) of Cosakievirus B3 (iCVB3), the signal sequence of human tissue plasminogen activator (tPA), the coding sequences, and two flanking spacers, between the permuted intron ends (Fig. 1a)[36]. The IRES facilitates cap-independent translation of the coding sequences, whereas the spacers allow the intron and IRES to fold properly[36]. circRNAs were produced by in vitro transcription (IVT) followed by PIE-mediated circularization reactions, and purified by high-performance liquid chromatography (HPLC) (Supplementary Fig. 1a–d). As expected, circRNAs were more resistant to RNase R digestion than their respective linear precursors (Supplementary Fig. 1e–g). The fragments covering the putative junction site were amplified and sequenced. The results confirmed the success and precision of circularization (Supplementary Fig. 1h). After transfection of human embryonic 293 T (HEK293T) cells with these circRNAs, we observed comparable expression of monomeric EDIII, EDIII-Fc, and EDIII-Fd in cell lysates, but monomeric EDIII appeared to be secreted into the culture media less efficiently than the other versions (Supplementary Fig. 1i). We also observed that HPLC purification enhanced the translation level of circRNAs encoding either enhanced green fluorescent protein (EGFP) or Firefly luciferases (Fluc) (Supplementary Fig. 1j, k).

To compare the immunogenicity of different forms of EDIII, we encapsulated the circRNAs with lipid nanoparticles (LNP) and intramuscularly (i.m.) administered them into 8-week-old female C57BL/6 mice (20 μg per mouse) (Fig. 1b). The encapsulation efficiency of each circRNA-LNP was greater than 90%, with an average diameter ranging from 83.7 to 87.3 nm (Supplementary Table 1). Seven days later, anti-E IgG antibodies were detectable in both EDIII-Fc- and EDIII-Fd-immunized mice but barely detectable in EDIII-immunized mice (Fig. 1c). At 2 weeks after injection, anti-E IgG titers increased by 3.7-fold in EDIII-Fc-immunized mice, by 1.7-fold in EDIII-Fd-immunized mice, but remained undetectable in 4 out of 12 EDIII-immunized mice (Fig. 1d). Accordingly, the titers of anti-ZIKV nAbs were approximately 7.5-fold higher in EDIII-Fc-immunized mice than in EDIII-Fd-immunized mice, but were undetectable in 10 out of 12 EDIII-immunized mice (Fig. 1e), suggesting that EDIII-Fc circRNA elicits higher titers of IgG and nAbs than EDIII-Fd and EDIII circRNAs.

Given the crucial roles of germinal center (GC) in B cell clonal expansion and antibody affinity maturation[37], we tested the GC reactions in the inguinal lymph nodes (ILNs) (Supplementary Fig. 2a, b). At 2 weeks after injection, follicular helper T (Tfh) cells and activated GL7$^+$ GC B cells were elicited more robustly in EDIII-Fc-immunized mice than in EDIII-Fd-immunized mice, but were not significantly elicited in EDIII-immunized mice (Fig. 1f, g). High frequencies of Tfh cells, known for providing critical helper signals to GC B cells[37], may contribute to the high antibody responses observed in EDIII-Fc-immunized mice. Consistently, at this time point, plasma cells were significantly higher in EDIII-Fc-immunized mice than in the mice immunized with EDIII-Fd or EDIII (Fig. 1h). Hence, EDIII-Fc circRNA elicits GC reactions more effectively than EDIII-Fd and EDIII circRNAs.

To determine whether these circRNAs also elicited T cell responses, we examined the cytokine-secreting profiles of splenic CD4$^+$ and CD8$^+$ T cells upon stimulation with ZIKV E-specific peptide pools (Supplementary Fig. 2c). At 2 weeks after injection, the frequencies of EDIII-specific CD4$^+$ T cells secreting interferon-γ (IFN-γ), tumor necrosis factor α (TNFα), or interleukin-2 (IL-2) were higher in

https://doi.org/10.1038/s41467-024-53242-0

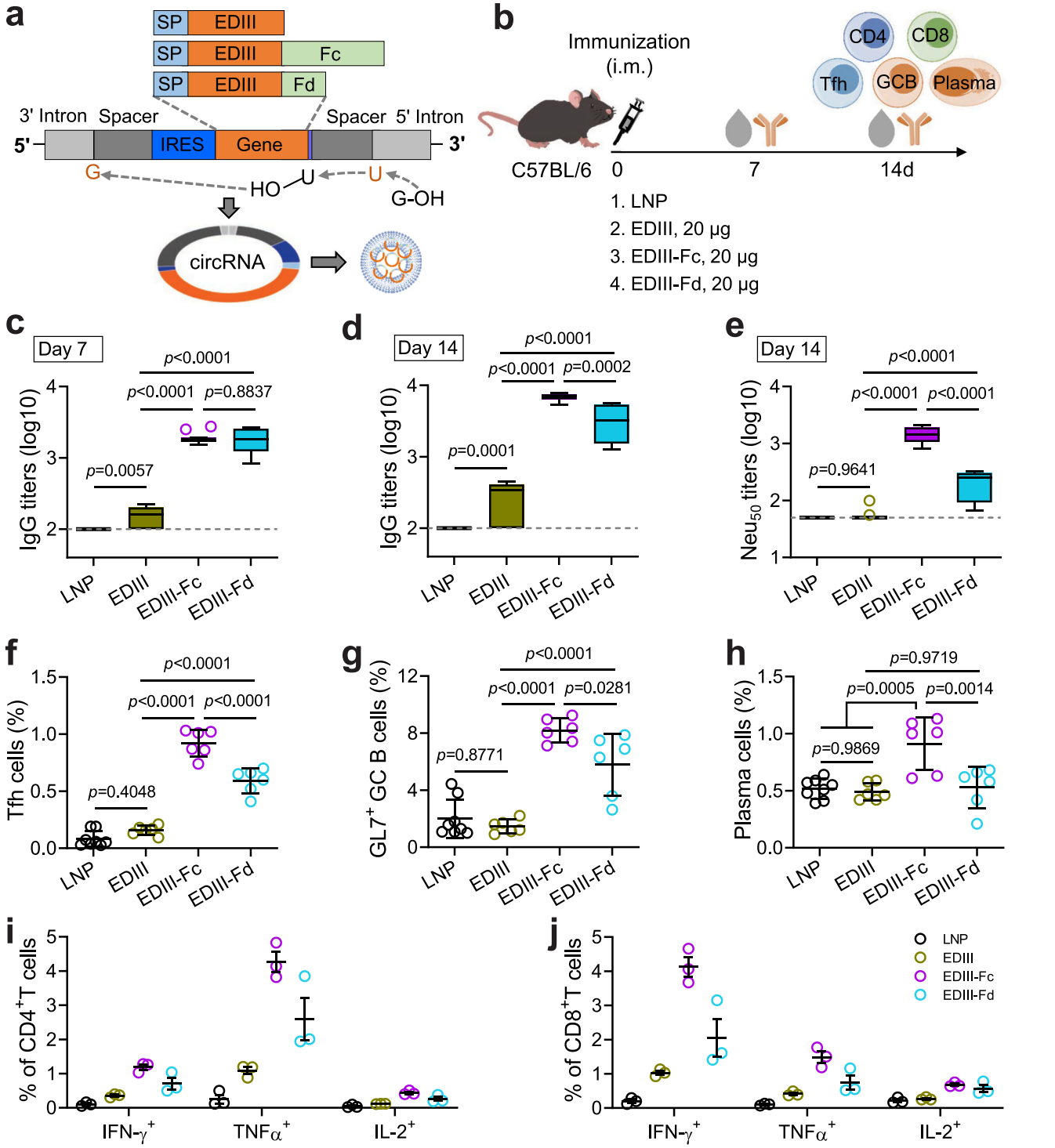

Fig. 1 | Immunogenicity of circRNAs encoding EDIII, EDIII-Fc, or EDIII-Fd. **a** Schematic diagram of PIE (Ana)-mediated RNA circularization. Coding sequences for EDIII, EDIII-Fc and EDIII-Fd were fused with tPA signal sequence at the 5′ termini and cloned into circRNA plasmids (Supplementary Fig. 1a). circRNAs were produced by IVT followed by circularization in the presence of GTP and Mg^{2+}. **b** Schematic diagram of immunization assay. **c**, **d** Anti-E IgG titers at 7 (**c**) or 14 (**d**) days after immunization were measured by ELISA. Titers were calculated as the reciprocals of the highest dilutions at which the optical density values at 450 nm (OD450) were equal to or higher than cut-off values. Limits of detection (LODs) are 100 and marked by gray dashed lines. **e** anti-ZIKV nAb titers at 14 days after immunization were measured by flow cytometry-based neutralization test (FNT) and calculated as the dilutions at which the percentages of ZIKV-positive cells were reduced to 50% of negative controls. LOD is 50. **f**–**h** Frequencies of Tfh cells in $CD4^+$ T cells (**f**), activated $GL7^+$ GC B cells in $CD38^-$ B cells (**g**) and plasma cells in lymphocytes (**h**) in the ILNs. At 14 days after immunization, ILN lymphocytes were isolated, labeled with surface marker antibodies, and measured by flow cytometry. **i**, **j** Frequencies of $CD4^+$ T (**i**) and $CD8^+$ T (**j**) cells secreting IFN-γ, TNFα, or IL-2. At 14 days after immunization, splenic lymphocytes were isolated, stimulated with ZIKV E peptide pools, and measured by intracellular cytokine staining assays. Box plots (**c**–**e**) indicate median (middle line), 25-75 percentile (box), 5-95 percentile (whiskers) and outliers (single points). Data points represent values for individual mice (**f**–**h**) or three technical replicates of pooled lymphocytes (**i**, **j**). n = 12 for (**c**–**e**). n = 8 (LNP) and 6 (EDIII, EDIII-Fc, EDIII-Fd) for (**f**–**h**). n = 3 for (**i**, **j**). Data are representative of two independent experiments and presented as mean ± standard derivation (s.d.). Comparisons are performed by one-way analysis of variation (ANOVA) and Tukey's multiple comparison tests. *p* values are shown on the graphs. Source data are provided as a Source Data file.

EDIII-Fc-immunized mice than in EDIII-Fd-immunized mice, and were barely detectable in EDIII-immunized mice (Fig. 1i). IL-2$^+$ CD4$^+$ T cells are essential for CD8$^+$ T cell activation at priming, whereas IFN-γ$^+$ and TNFα$^+$ CD4$^+$ T cells promote CD8$^+$ T cell proliferation and cytokine production[38]. Indeed, we observed higher frequencies of CD8$^+$ T cells secreting IFN-γ, TNFα, or IL-2 in EDIII-Fc-immunized mice than in either EDIII-Fd- or EDIII-immunized mice (Fig. 1j). EDIII-Fc circRNA is thus better than EDIII-Fd and EDIII circRNAs in inducing Th1-biased T cell responses.

EDIII-Fc circRNA alone partially protects against ZIKV infection

To assess the protective effects of EDIII-Fc and EDIII-Fd circRNAs in neonatal mice through passive maternal immunity, we i.m. immunized 8-week-old female C57BL/6 mice twice with 20 μg circRNA at a 3-week interval (Fig. 2a). After each immunization, EDIII-Fc circRNA elicited significantly higher titers of anti-ZIKV nAbs than EDIII-Fd circRNA (Fig. 2b). At 2 weeks after the final immunization, the immunized female mice were mated. After birth, 1-day-old pups were subcutaneously (s.c.) challenged with 1×10^4 focus-forming-units (FFU) of ZIKV (GZ02 strain). All pups born to phosphate buffered saline (PBS)-immunized mice showed severe growth delay and died within 15 days (Fig. 2c and Supplementary Fig. 3a). In contrast, pups born to EDIII-Fc-immunized mice showed mild growth delay and all survived, whereas those born to EDIII-Fd-immunized mice showed moderate growth delay and 7 out of 16 pups survived (Fig. 2c and Supplementary Fig. 3a). Both EDIII-Fc and EDIII-Fd circRNAs effectively inhibited the ZIKV-caused neurological disorders, including paralysis of limbs and tail and retardation of brain growth (Fig. 2d and Supplementary Fig. 3b), with EDIII-Fc circRNA achieving a greater inhibition. EDIII-Fc circRNA also outperformed EDIII-Fd circRNA in reducing the brain viral loads (Fig. 2e), and in inhibiting meningeal lymphocyte infiltration and cortex laminar necrosis (Fig. 2f, g). Thus, compared to EDIII-Fd circRNA, maternal immunization with EDIII-Fc circRNA confers better protection against ZIKV challenge in the offspring.

To assess the protective effects of these circRNAs in adult mice by active immunization, we i.m. immunized 12-week-old *Ifnar*$^{-/-}$ C57BL/6 mice twice with 20 μg circRNA at a 3-week interval (Fig. 2h). In this line of mouse, EDIII-Fc circRNA still elicited higher titers of anti-E IgG and nAbs than EDIII-Fd circRNA (Fig. 2i and Supplementary Fig. 3c), consistent with the observations in wild-type C57BL/6 mice (Fig. 1c–e and Fig. 2b). At 3 weeks after the final immunization, we s.c. challenged the mice with 1×10^5 FFU of ZIKV. PBS-immunized mice showed severe body mass loss and all died within 10 days, whereas both EDIII-Fc- and EDIII-Fd-immunized mice showed moderate body mass loss and all survived (Fig. 2j and Supplementary Fig. 3d). EDIII-Fc circRNA was more efficacious than EDIII-Fd circRNA in reducing the viral loads in the sera, brains and spleens (Fig. 2k and Supplementary Fig. 3e, f). Together, in both challenge models, EDIII-Fc circRNA confers better protection than EDIII-Fd circRNA, but neither alone is sufficient to confer complete protection.

Combining EDIII-Fc and NS1 circRNAs improves protective effects

We next aimed to improve the protective effects by incorporating NS1[39]. Using the Ana PIE method, we successfully produced NS1 circRNA, enabling effective expression of dimeric NS1 in transfected HEK293T cells (Supplementary Fig. 4). We combined equal masses of circRNAs encoding EDIII-Fc and NS1 into two distinct formulations: EN(LNP) and EN(RNA). EN(LNP) is a cocktail of LNPs encapsulating EDIII-Fc circRNA and NS1 circRNA separately. EN(RNA) consists of LNPs encapsulating a pre-mixed blend of EDIII-Fc and NS1 circRNAs. Following i.m. administration in C57BL/6 mice (Fig. 3a), both EN(LNP) and EN(RNA) induced comparable titers of anti-E IgG and nAbs, similar to those induced by EDIII-Fc circRNA alone, and comparable titers of anti-NS1 IgG as induced by NS1 circRNA alone (Fig. 3b and Supplementary Fig. 5a, b), revealing no antigenic competition existing between EDIII-Fc and NS1. A single-dose maternal immunization with either EN(LNP) or EN(RNA) fully protected the pups against the ZIKV-caused growth delay (Fig. 3c), mortality (Fig. 3d), paralysis of limbs and tail (Fig. 3e), and brain growth retardation (Supplementary Fig. 5c). Maternal immunization with either EN(LNP) or EN(RNA) eradicated viral infection in the brains of 4 or 3 out of 7 pups, respectively (Fig. 3f). A single dose of either circRNA alone mitigated, but not prevented, the ZIKV-caused growth delay (Fig. 3c), mortality (Fig. 3d), neurological symptoms (Fig. 3e), and viral infection in neonatal brains (Fig. 3f), with EDIII-Fc circRNA showing marginally superior efficacy over NS1 circRNA. Pups born to either EN(LNP)- or EN(RNA)-immunized mice showed no meningeal lymphocyte infiltration or cortical laminar necrosis, whereas pups born to EDIII-Fc- or NS1-immunized mice showed signs of meningeal inflammation and cortical laminar necrosis, albeit to a lesser degree than pups born to PBS-immunized mice (Fig. 3g, h). Thus, the combination of EDIII-Fc and NS1 circRNAs, regardless of the formulation, provides better protection against the ZIKV-caused symptoms and brain damage in the neonates than each circRNA singly.

To determine whether an additional dose could prevent ZIKV infection in neonatal brains, we administered a booster of each vaccine to the mice 3 weeks after the first dose (Fig. 4a). Two weeks after the booster immunization, we observed a significant increase in the titers of anti-E IgG, anti-NS1 IgG, and nAbs (Fig. 4b and Supplementary Fig. 5d, e). Both EN(LNP) and EN(RNA) prevented the ZIKV-caused growth delay (Fig. 4c), mortality (Fig. 4d), neurological symptoms (Fig. 4e), and brain growth retardation (Supplementary Fig. 5f), and eliminated viral infection in all but one pup in the EN(RNA) group (Fig. 4f), revealing significantly improved protective effects. EDIII-Fc circRNA effectively prevented the ZIKV-caused growth delay and mortality, mitigated neurological disorders, and reduced but failed to eradicate ZIKV infection in neonatal brains (Fig. 4c–f and Supplementary Fig. 5f). NS1 circRNA also prevented mortality, reduced growth delay and neurological disorders, but could not significantly reduce brain viral loads (Fig. 4c–f and Supplementary Fig. 5f). In line with these findings, EN(LNP) and EN(RNA) effectively inhibited the ZIKV-caused meningeal inflammation and cortical laminar necrosis, whereas either EDIII-Fc circRNA or NS1 circRNA greatly reduced, but not eliminated, the ZIKV-cause brain damage (Fig. 4g, h). Thus, the combination of EDIII-Fc and NS1 circRNAs, especially the EN(LNP) formulation, have the potential to confer full protection, but two doses are desirable.

To further assess the protective effects of EN(LNP) and EN(RNA) in adult mice and how quickly they took effect, we i.m. immunized 12-week-old *Ifnar*$^{-/-}$ mice with each vaccine (Supplementary Fig. 6a). Ten days later, EN(LNP) and EN(RNA) elicited anti-E and anti-NS1 IgG at comparable levels as those elicited by either circRNA alone (Supplementary Fig. 6b, c). By this time, nAbs were detectable in 2 out of 6 EN(LNP)-immunized mice (Supplementary Fig. 6d). Following a s.c. challenge with 1×10^5 FFU of ZIKV on day 12, PBS-immunized mice showed severe body mass loss, with all but one succumbing to the infection (Supplementary Fig. 6e, f). In contrast, both EN(LNP)- and EN(RNA)-immunized mice experienced a transient body mass loss during days 6-8 post-challenge, yet all eventually recovered. Mice receiving either circRNA alone showed moderate body mass loss and all but one survived (Supplementary Fig. 6e, f). All these vaccines, except NS1 circRNA, significantly reduced serum viral loads (Supplementary Fig. 6g). Hence, both EN(LNP) and EN(RNA) have the potential to confer rapid protection against fatal ZIKV infection in adult *Ifnar*$^{-/-}$ mice.

circRNA immunization does not enhance DENV2 infection in mice

E-specific cross-reactive antibodies with low or no neutralizing activities may cause ADE[7]. We thus examined the cross-reactivity of

https://doi.org/10.1038/s41467-024-53242-0

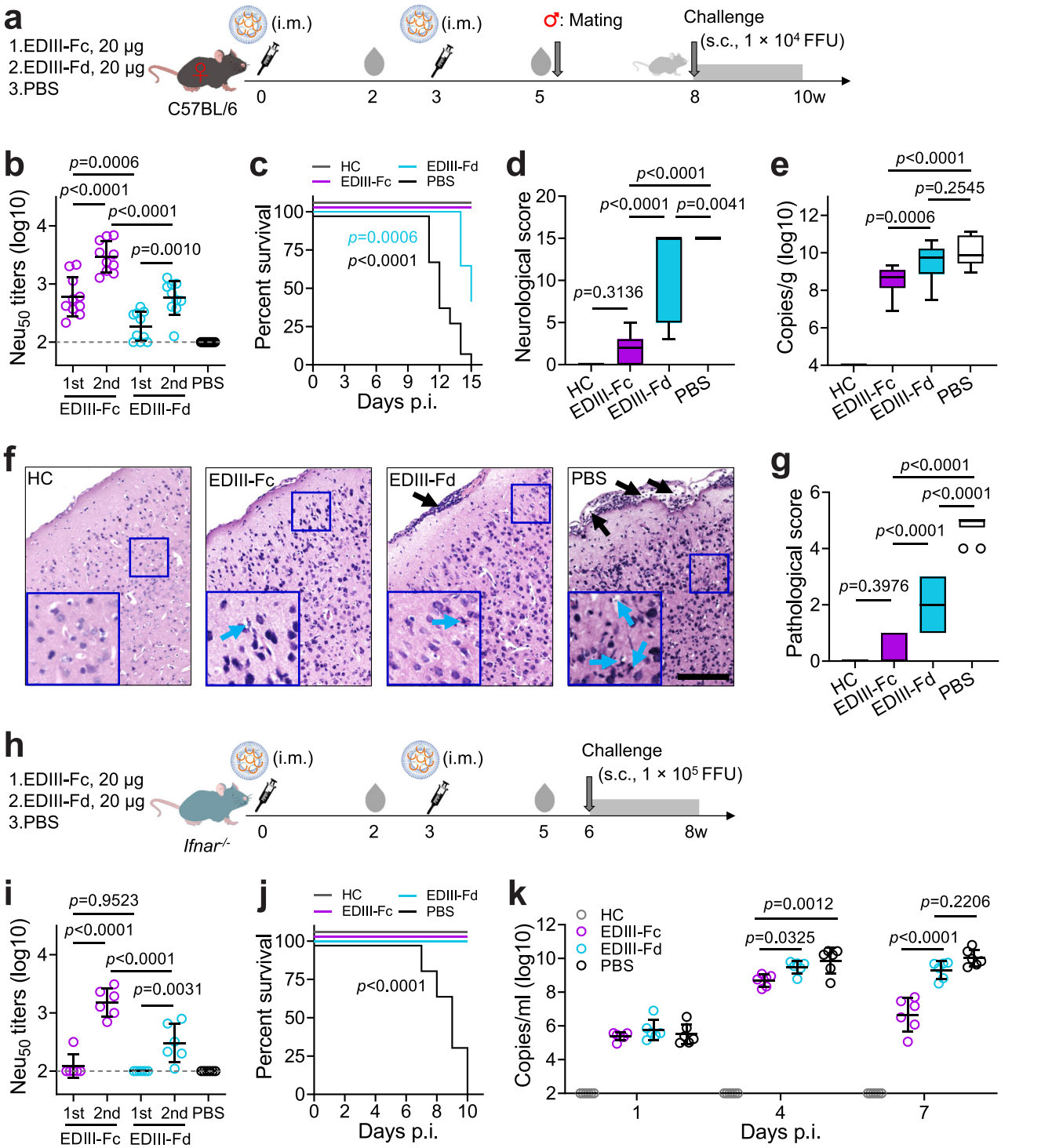

Fig. 2 | Protective effects of EDIII-Fc and EDIII-Fd circRNAs. a Schematic diagram of maternal immunization and neonatal challenge model. Eight-week-old female C57BL/6 mice were i.m. immunized twice with each circRNA and mated at 2 weeks after the final immunization. One-day-old pups were s.c. challenged with 1×10^4 FFU of ZIKV. Fifteen days later, pups were sacrificed. **b** anti-ZIKV nAb titers in C57BL/6 mice at 2 weeks after each immunization. LOD is 100 and marked by gray dashed line. **c** Survival curves of the pups. **d** Neurological scores of the pups at 15 days after challenge. Paralysis of limbs and tail were scored in a single-blind manner. Maximum severity and death received scores of 14 and 15, respectively. **e** ZIKV genome copies in neonatal brains at 15 days after challenge or at sacrifice. **f** H&E staining of brain tissue sections. Representative images are shown. Black arrows, meningeal lymphocyte infiltration. Cyan arrows, necrotic cells in cortex. Scale bar = 100 μm. **g** Pathological scores of neonatal brains. Meningeal lymphocyte infiltration and cortex laminar necrosis were scored in a single-blind manner. **h** Schematic diagram of immunization and challenge assay in *Ifnar*$^{-/-}$ mice. Twelve-week-old mice were immunized twice and challenged with 1×10^5 FFU of ZIKV. **i** anti-ZIKV nAb titers at 2 weeks after each immunization. **j** Survival curves. **k** ZIKV genome copies in the sera at 1, 4, and 7 days after challenge. Box plots (**d**, **e**, **g**) indicate median (middle line), 25–75 percentile (box), 5-95 percentile (whiskers) and outliers (single points). Data points represent mean values of two (**b**, **i**) or three (**k**) technical replicates for one mouse. n = 10 for (**b**). n = 13 (Healthy control, HC), 14 (EDIII-Fc), 16 (EDIII-Fd) and 10 (PBS) for (**c**–**g**). n = 6 for (**i**–**k**). Data are representative of two independent experiments and presented as mean ± s.d. Comparisons were performed between each group and HC by Log-rank (Mantel-Cox) test (**c**, **j**). Other comparisons were performed by one-way ANOVA and Tukey's multiple comparison tests. *p* values are shown on the graphs. Source data are provided as a Source Data file.

https://doi.org/10.1038/s41467-024-53242-0

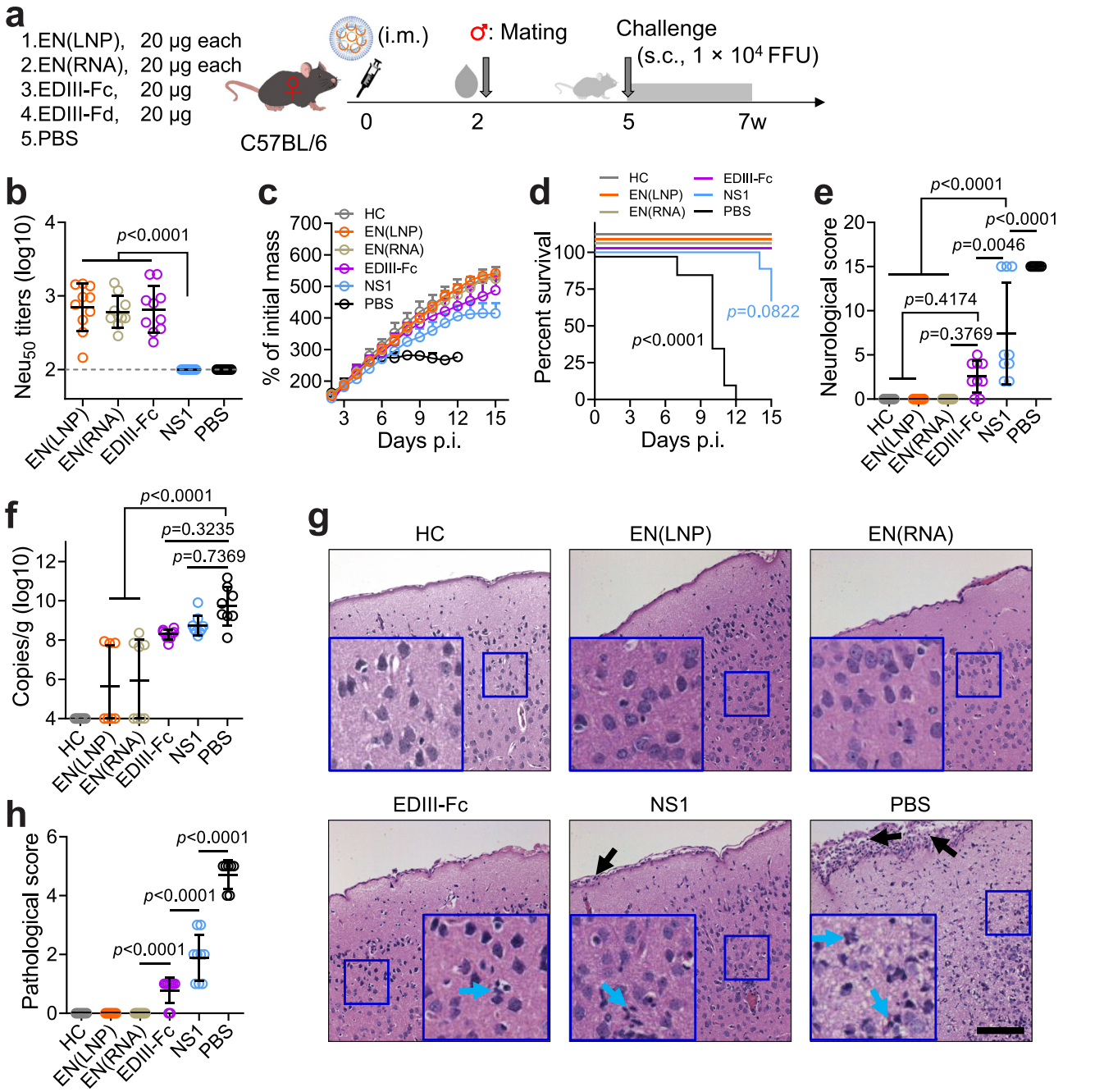

Fig. 3 | Immunogenicity and protective efficacy of a single-dose immunization with the combination of EDIII-Fc and NS1 circRNAs in ZIKV-infected neonatal mouse model. a Schematic diagram of maternal immunization and neonatal challenge model. Eight-week-old female C57BL/6 mice were i.m. immunized once with the indicated vaccines at 20 μg each circRNA per mouse or an equal volume of PBS. Immunized mice were mated at 2 weeks after immunization. After birth, 1-day-old pups were s.c. challenged with 1×10^4 FFU of ZIKV. Fifteen days later, pups were sacrificed. **b** anti-ZIKV nAb titers in C57BL/6 mice at 2 weeks after immunization. LOD is 100 and marked by gray dashed line. **c** Growth curves of the pups. **d** Survival curves of the pups. **e** Neurological scores of the pups at 15 days after challenge. **f** ZIKV genome copies in neonatal brains at 15 days after challenge or at sacrifice. **g** H&E staining of brain tissue sections. Representative images of each group are shown. Black arrows, meningeal lymphocyte infiltration. Cyan arrows, necrotic cells in cortex. Scale bar = 50 μm. **h** Pathological scores of neonatal brains. Meningeal lymphocyte infiltration and cortex laminar necrosis were scored in a single-blind manner. Data points represent mean values of two (**b**) or three (**f**) technical replicates for one mouse, or mean values of one group (**c**), or values for individual mice (**e**, **h**). n = 10 for (**b**). n = 7 (HC, EN(LNP)), 8 (EN(RNA), PBS) and 9 (EDIII-Fc, NS1) for (**c**–**h**). Data are representative of two independent experiments and presented as mean ± s.d. Comparisons were performed between each group and HC by Log-rank (Mantel-Cox) test (**d**). Other comparisons were performed by one-way ANOVA and Tukey's multiple comparison tests. *p* values are shown on the graphs. Source data are provided as a Source Data file.

the immune sera to DENV EDIII (DENV1) or E (DENV2-4) proteins. Compared to mice sera collected at 2 weeks after ZIKV infection (ZIKV sera), which showed binding activities to ZIKV and all four DENVs, EDIII-Fc sera showed higher binding activities to ZIKV but much lower to DENVs, with more than half of EDIII-Fc sera showing no DENV-reactivity (Fig. 5a). Both EN(LNP) sera and EN(RNA) sera also showed comparable or higher ZIKV-binding activities but significantly lower DENV-binding activities compared to ZIKV sera. NS1 sera did not recognize the EDIII or E proteins of either ZIKV or DENV (Fig. 5a). Notably, the DENV-reactive antibodies in EN(LNP)-

https://doi.org/10.1038/s41467-024-53242-0

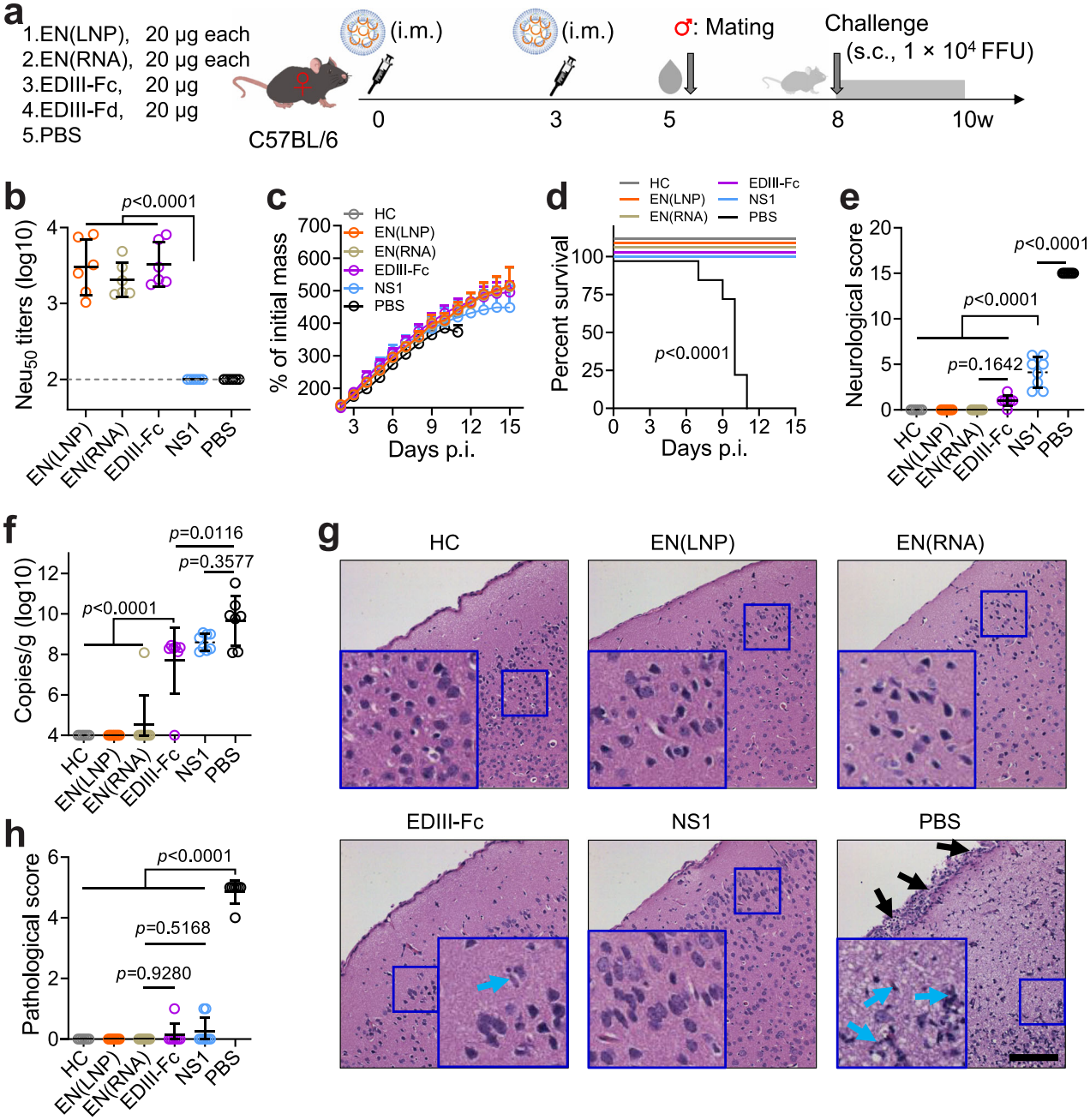

Fig. 4 | Immunogenicity and protective efficacy of a two-dose immunization with the combination of EDIII-Fc and NS1 circRNAs in ZIKV-infected neonatal mouse model. a Schematic diagram of maternal immunization and neonatal challenge model. Eight-week-old female C57BL/6 mice were i.m. immunized twice with the indicated vaccines at 20 μg each circRNA per mouse at a 3-week interval. Immunized mice were mated at 2 weeks after the final immunization. After birth, 1-day-old pups were s.c. challenged with 1×10^4 FFU of ZIKV. Fifteen days later, pups were sacrificed. **b** anti-ZIKV nAb titers in C57BL/6 mice at 2 weeks after the final immunization. LOD is 100 and marked by gray dashed line. **c** Growth curves of the pups. **d** Survival curves of the pups. **e** Neurological scores of the pups at 15 days after challenge. **f** ZIKV genome copies in neonatal brains at 15 days after challenge or at sacrifice. **g** H&E staining of brain tissue sections. Representative images of each group are shown. Black arrows, meningeal lymphocyte infiltration. Cyan arrows, necrotic cells in cortex. Scale bar = 50 μm. **h** Pathological scores of neonatal brains. Meningeal lymphocyte infiltration and cortex laminar necrosis were scored in a single-blind manner. Data points represent mean values of two (**b**) or three (**f**) technical replicates for one mouse, or mean values of one group (**c**), or values for individual mice (**e**, **h**). n = 6 for (**b**). n = 6 (HC), 7 (EDIII-Fc) and 8 (EN(LNP), EN(RNA), NS1, PBS) for (**c**–**e**). n = 6 (HC), 7 (EDIII-Fc, PBS) and 8 (EN(LNP), EN(RNA), NS1) for (**f**–**h**). Data are representative of two independent experiments and presented as mean ± s.d. Comparisons of survival rates between each group and HC were performed by Log-rank (Mantel-Cox) test (**d**). Other comparisons were performed by one-way ANOVA and Tukey's multiple comparison tests. *p* values are shown on the graphs. Source data are provided as a Source Data file.

immunized mice declined to be barely detectable within 10 weeks, whereas those in ZIKV-infected mice remained high for at least 12 weeks (Supplementary Fig. 7), suggesting that EDIII-Fc, alone or combined with NS1, elicits minimal and transient DENV-reactive antibodies.

To determine whether the immune sera had any ADE effects in cell cultures, ZIKV and DENV were incubated with ZIKV sera or immune sera and subsequently used to infect FcγR-bearing K562 cells. Without antibodies, this cell line is not susceptible to infection by ZIKV or DENV. ZIKV sera, but not NS1 sera, significantly promoted the infection

https://doi.org/10.1038/s41467-024-53242-0

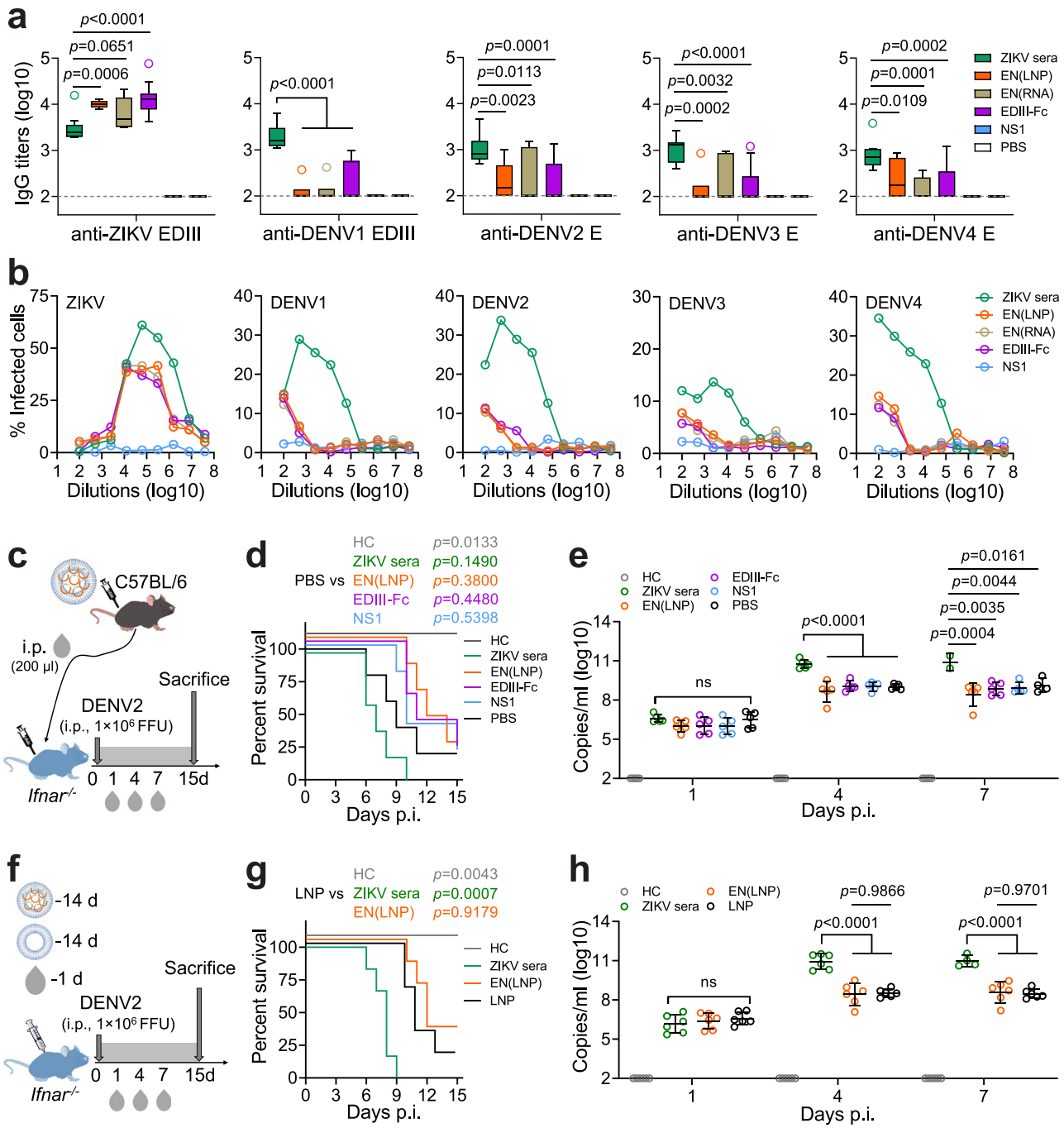

Fig. 5 | ADE risks of prototype circRNA vaccines in mice. a Cross-reactivity of immune sera to ZIKV and DENV. Mice sera were serially diluted and tested by ELISA using EDIII of ZIKV and DENV1, or E of DENV2, DENV3, and DENV4. LOD is 100 and marked by gray dashed line. Box plots indicate median (middle line), 25-75 percentile (box), 5-95 percentile (whiskers) and outliers (single points). **b** In vitro ADE activities of immune sera. Equally pooled mice sera in each group were 5-fold serially diluted (starting at 1:100) and incubated with ZIKV or DENV. The mixtures were used to infect K562 cells. Infected cells were examined by flow cytometry using anti-ZIKV mAb 8D10 or a cross-reactive mAb ZK8-4. **c** In vivo ADE activities of immune sera. Equally pooled mice sera in each group were diluted tenfold with PBS. Twelve-week-old *Ifnar*$^{-/-}$ mice were i.p. transferred with 200 µl diluted sera 1 day before i.p. challenge with 1×10^6 FFU of mouse-adapted DENV2. **d** Survival curves. **e** DENV2 genome copies in the sera at 1, 4, and 7 days after challenge. **f** In vivo ADE activities of circRNA immunization. Twelve-week-old *Ifnar*$^{-/-}$ mice were i.m. immunized with EN(LNP) or empty LNPs 2 weeks before challenge. Mice receiving 200 µl diluted ZIKV sera 1 day before challenge were used as controls. **g** Survival curves. **h** DENV2 genome copies in the sera at 1, 4, and 7 days after challenge. Data points represent mean values of three technical replicates for one mouse (**e**, **h**). n = 10 (ZIKV sera), 16 (EDIII-Fc) and 6 (EN(LNP), EN(RNA), NS1, PBS) for (**a**). n = 5 for (**c**–**e**). n = 6 for (**f**–**h**). Data are representative of at least two independent experiments and presented as mean ± s.d. Comparisons were performed by unpaired two-tailed Student's t-test between each group and ZIKV sera group (**a**), Log-rank (Mantel-Cox) tests between PBS (**d**) or LNP group (**g**) and the rest groups, or by one-way ANOVA and Tukey's multiple comparison tests (**e**, **h**). *p* values are shown on the graphs. Source data are provided as a Source Data file.

of DENV at dilutions ranging from 1:100 to 1:62500 (Fig. 5b). In contrast, EN(LNP), EN(RNA) or EDIII-Fc sera slightly promoted DENV infection only at dilutions below 1:2500 (Fig. 5b). Thus, EDIII-Fc, alone or combined with NS1, elicits minimal, if any, ADE-prone antibodies.

To determine whether the immune sera had any ADE effects on DENV infection in mice, we established a mouse-adapted DENV2 variant by alternating the passaging of DENV2 strain 16681 between Vero cells and 1-day-old C57BL/6 mice across 3 cycles. Compared to the parental strain, the variant (GenBank No. PQ008452) harbored 3 nonsynonymous mutations (NS1 K174N, NS2A L181V, and NS5 A196T) and caused more rapid deaths in 1-day-old ICR mice (Supplementary Fig. 8a–c), revealing enhanced virulence in mice. We intraperitoneally (i.p.) inoculated 200 µl tenfold diluted ZIKV sera or immune sera into *Ifnar*$^{-/-}$ mice 1 day before challenge with DENV2 variant at 1×10^6 FFU per mouse (Fig. 5c). Compared to mice receiving PBS, those receiving ZIKV sera showed more severe body mass loss upon DENV2 challenge (Supplementary Fig. 8d), and rapidly succumbed to infection (Fig. 5d). ZIKV sera increased the serum viral loads by 1.6-2.5 log (Fig. 5e), revealing a significant enhancement of DENV2 infection in mice. In contrast, none of the immune sera aggravated the DENV2-caused body mass loss or mortality, or increased the serum viral loads (Fig. 5d, e and Supplementary Fig. 8d), suggesting that at the tested doses, the immune sera unlikely promote DENV2 infection in mice as ZIKV sera do.

To further determine whether an active immunization with EN(LNP) caused ADE of DENV2 infection, we i.m immunized *Ifnar*$^{-/-}$ mice once with EN(LNP) (20 µg each circRNA) or an equivalent mass of empty LNPs 14 days before DENV2 challenge (Fig. 5f). Mice that received a transfer of 200 µl diluted ZIKV sera served as controls. Unlike ZIKV sera that enhanced DENV2 infection and mortality, EN(LNP) immunization did not enhance the DENV2-caused body mass loss, mortality, or serum viral loads compared to empty LNPs (Fig. 5g, h and Supplementary Fig. 8e). Together, at the tested settings, EN(LNP) immunization unlikely causes ADE of DENV2 infection in mice.

A single dose of optimized circRNA vaccine confers potent protection

The effectiveness of a circRNA vaccine partially depends on the quantity of antigens it produces. We thus refined the circRNA backbone to elevate the translation. We utilized the IRES of human rhinovirus B3 (iHRV-B3) due to its superior translation efficiency compared to iCVB3 in circRNAs[40]. We also introduced an RNA-binding motif for human poly(A)-binding protein (PABP) into the 5′ upstream of iHRV-B3, inserted an eIF4G-recruiting aptamer (Apt-eIF4G) at the proximal loop of domain IV of iHRV-B3, and added the 3′ UTR of human α-globin 1 (HBA1) mRNA into the 3′ downstream of the stop codon (Fig. 6a and Supplementary Fig. 9a). These elements have been shown to elevate the translational activity of circRNAs[40]. We synthesized the optimized circRNAs using the PIE method based on the group I catalytic intron of bacteriophage T4 Td gene (T4 Td) (Supplementary Fig. 9b–e)[40]. Through these modifications, we achieved a notable increase in protein production, including EDIII-Fc, NS1, and Gaussia luciferase (Gluc, ~4.5-fold), as observed in transfection assays (Fig. 6b and Supplementary Fig. 9f). Compared to nucleotide-modified linear mRNAs coding for the same EDIII-Fc and NS1, optimized circRNAs showed somewhat lower levels of translation (Supplementary Fig. 10a).

We comparatively assessed the immunogenicity of optimized circRNAs and their respective linear mRNA counterparts in C57BL/6 mice (Supplementary Fig. 10b). At 2 weeks after immunization, optimized circRNAs, encoding either EDIII-Fc or NS1 or their combination, elicited lower levels of anti-E IgG (1.8- to 2.4-fold), anti-NS1 IgG (3.4- to 3.9-fold), and nAbs (2.0- to 3.5-fold) than linear mRNAs (Supplementary Fig. 10c–e). Optimized circRNAs, except that encoding EDIII-Fc, elicited slightly weaker Tfh response than linear mRNAs (Supplementary Fig. 10f). The frequencies of activated GC B cells appeared to be comparable in mice receiving optimized circRNAs or linear mRNAs, and so did the plasma cells (Supplementary Fig. 10g, h). Given that EN(LNP) showed immunogenicity and protective efficacy comparable to EN(RNA) while the formulation was easier (Figs. 3, 4 and Supplementary Fig. 5), we selected optimized EN(LNP) for further evaluation. We i.m. immunized 8-week-old female C57BL/6 mice once with prototype or optimized EN(LNP) (designated as P and Opt, respectively) at 5 or 20 µg each circRNA per mouse (Fig. 6c). Compared to prototype EN(LNP), optimized EN(LNP) elicited significantly higher titers of IgG and nAbs at each tested dose (Fig. 6d and Supplementary Fig. 11a, b). Thus, optimization of the circRNAs effectively improves their immunogenicity, albeit still being weaker than that of linear mRNAs at the tested doses and timeframe (Supplementary Fig. 10c–e).

We then challenged the pups born to mice that received a single dose of prototype or optimized EN(LNP) (Fig. 6c). A high dose of optimized EN(LNP) prevented the ZIKV-caused growth delay (Supplementary Fig. 11c), mortality (Fig. 6e), neurological symptoms (Fig. 6f), brain growth retardation (Supplementary Fig. 11d), and viral infection in neonatal brains (Fig. 6g). A high dose of prototype EN(LNP) also prevented the ZIKV-caused diseases (Fig. 6e–g and Supplementary Fig. 11c, d), but viral genomes remained detectable in 5 out of 12 pups (Fig. 6g). At the low dose, optimized EN(LNP) still showed better protection than prototype EN(LNP), evidenced by the faster body growth, no mortality, milder symptoms and lower brain viral loads (Fig. 6e–g and Supplementary Fig. 11c, d). We observed meningeal inflammation and cortical laminar necrosis in 3 out of 15 pups born to mice receiving a low dose of prototype EN(LNP) but not in those born to mice receiving each dose of optimized EN(LNP) or a high dose of prototype EN(LNP) (Fig. 6h and Supplementary Fig. 11e). Together, a single-dose maternal immunization with optimized EN(LNP) completely protects against ZIKV infection in the offspring.

We also assessed the protective effects of optimized EN(LNP) in *Ifnar*$^{-/-}$ mice that received a single-dose immunization (Fig. 6i). Compared to a high dose of prototype EN(LNP) (20 µg each circRNA), an equal dose of optimized EN(LNP) elicited higher titers of IgG and nAbs, whereas a 4-fold lower dose of optimized EN(LNP) (5 µg each circRNA) elicited lower titers of IgG but comparable titers of nAbs (Fig. 6j and Supplementary Fig. 11f, g). After being challenged with ZIKV, all mice receiving a high dose of optimized EN(LNP) survived without body mass loss, in contrast to mice receiving a high dose of prototype EN(LNP) or a low dose of optimized EN(LNP), all of whom survived but experienced body mass loss (Fig. 6k and Supplementary Fig. 11h). In mice receiving a high dose of optimized EN(LNP), breakthrough infections were mostly cleared within 4 days (Fig. 6l). By contrast, mice receiving a high dose of prototype EN(LNP) or a low dose of optimized EN(LNP) showed viremia up to 7 days, albeit at lower levels than those receiving PBS (Fig. 6l). At 7 days after challenge, nAb titers showed a 1.6-fold increase in mice receiving a high dose of optimized EN(LNP), compared to 2.5- and 4.4-fold increases in the high-dose prototype group and low-dose optimized group, respectively (Supplementary Fig. 11i), consistent with the severity of their respective viremia. Thus, a single high dose of optimized EN(LNP) effectively protects against ZIKV infection in adult mice.

Protective immunity elicited by optimized circRNA vaccine is durable

To examine the durability of the protective immunity elicited by circRNA immunization, a desirable property for an ideal ZIKV vaccine, we i.m. immunized 8-week-old female C57BL/6 mice once with prototype or optimized EN(LNP) at 20 µg each circRNA per mouse (Fig. 7a). Optimized EN(LNP) constantly elicited higher titers of anti-ZIKV nAbs than prototype EN(LNP) at 4, 6, and 8 weeks after immunization (3.0- to 3.4-fold, Fig. 7b). At 11 weeks after immunization, we s.c. challenged the 1-day-old pups born to the immunized mice. Optimized EN(LNP) prevented the ZIKV-caused growth delay, mortality, neurological

https://doi.org/10.1038/s41467-024-53242-0

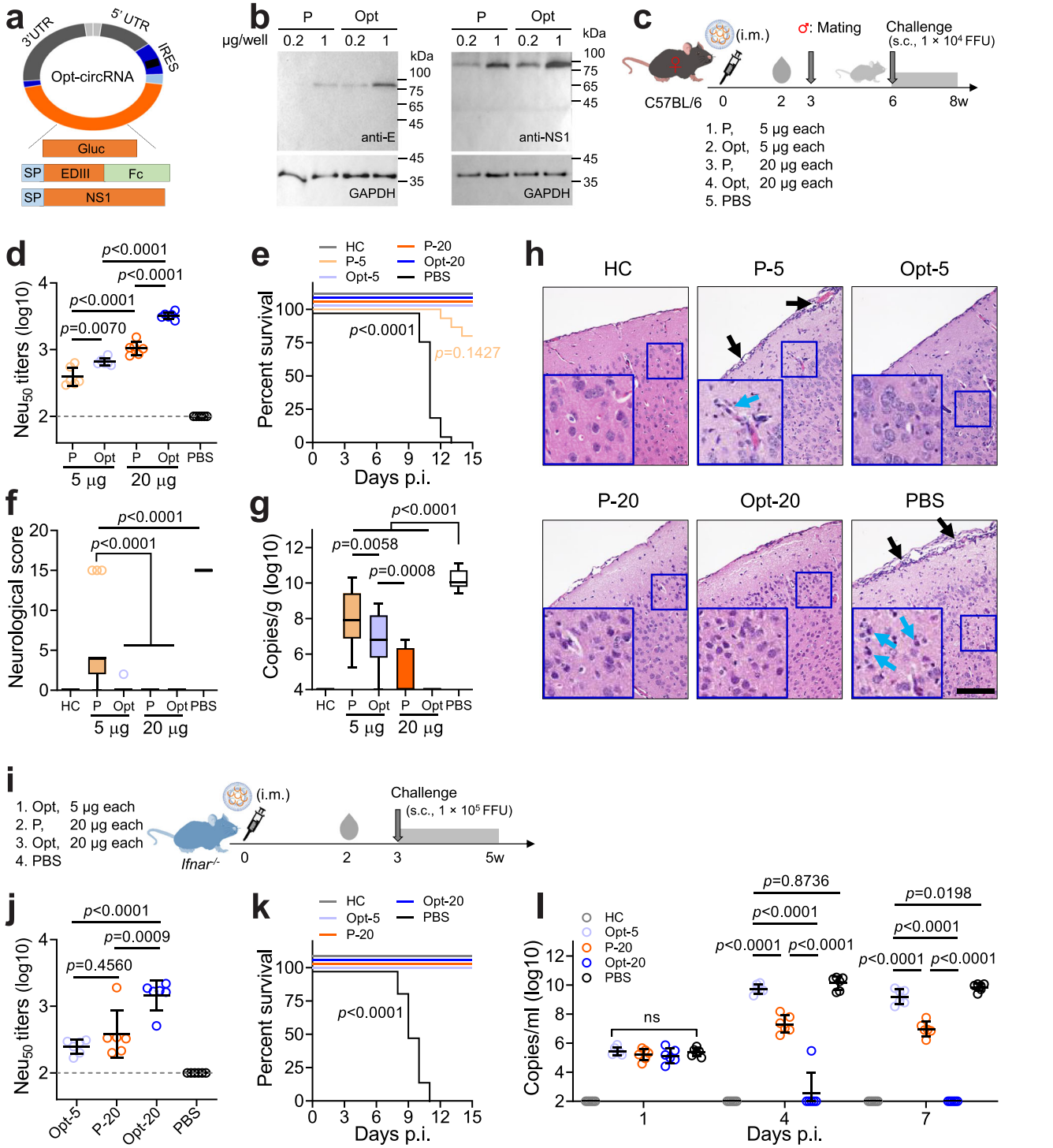

Fig. 6 | Immunogenicity and protective efficacy of optimized EN(LNP) in mice. **a** Schematic diagram of optimized circRNA. Detailed elements have been depicted in Supplementary Fig. 9a. **b** Western blot analysis of EDIII-Fc and NS1 in the culture media of HEK293T cells transfected with prototype (P) or optimized (Opt) circRNAs (without β-mercaptoethanol). Glyceraldehyde-3-phosphate dehydrogenase (GAPDH) in cell lysates was also examined. Analysis was independently repeated twice with similar results. **c** Vaccine doses and schedule for maternal immunization and neonatal challenge model. One-day-old pups were s.c. challenged with 1×10^4 FFU of ZIKV. Fifteen days later, pups were sacrificed. **d** anti-ZIKV nAb titers in C57BL/6 mice at 2 weeks after immunization. LOD is 100 and marked by gray dashed line. **e** Survival curves of the pups. **f** Neurological scores of the pups at 15 days after challenge. **g** ZIKV genome copies in neonatal brains at 15 days after challenge or at sacrifice. Box plots (**f**, **g**) indicate median (middle line), 25–75 percentile (box), 5-95 percentile (whiskers) and outliers (single points). **h** H&E staining of brain tissue sections. Representative images are shown. Black arrows, meningeal lymphocyte infiltration. Cyan arrows, necrotic cells in cortex. Scale bar = 100 μm. **i** Vaccine doses and schedule for immunization and challenge assay in *Ifnar*$^{-/-}$ mice. Fifteen days after challenge, mice were sacrificed. **j** anti-ZIKV nAb titers in *Ifnar*$^{-/-}$ mice at 2 weeks after immunization. **k** Survival curves. **l**, ZIKV genome copies in the sera at 1, 4, and 7 days after challenge. Data points represent mean values of two (**d**, **j**) or three (**l**) technical replicates for one mouse. n = 6 for (**d**). n = 10 (HC), 15 (P-5), 12 (P-20) and 14 (Opt-5, Opt-20, PBS) for (**e**–**h**). n = 6 for (**j**–**l**). Data are representative of two independent experiments and presented as mean ± s.d. Comparisons of survival rates between each group and HC were performed by Log-rank (Mantel-Cox) test (**e**, **k**). Other comparisons were performed by one-way ANOVA and Tukey's multiple comparison tests. *p* values are shown on the graphs. Source data are provided as a Source Data file.

https://doi.org/10.1038/s41467-024-53242-0

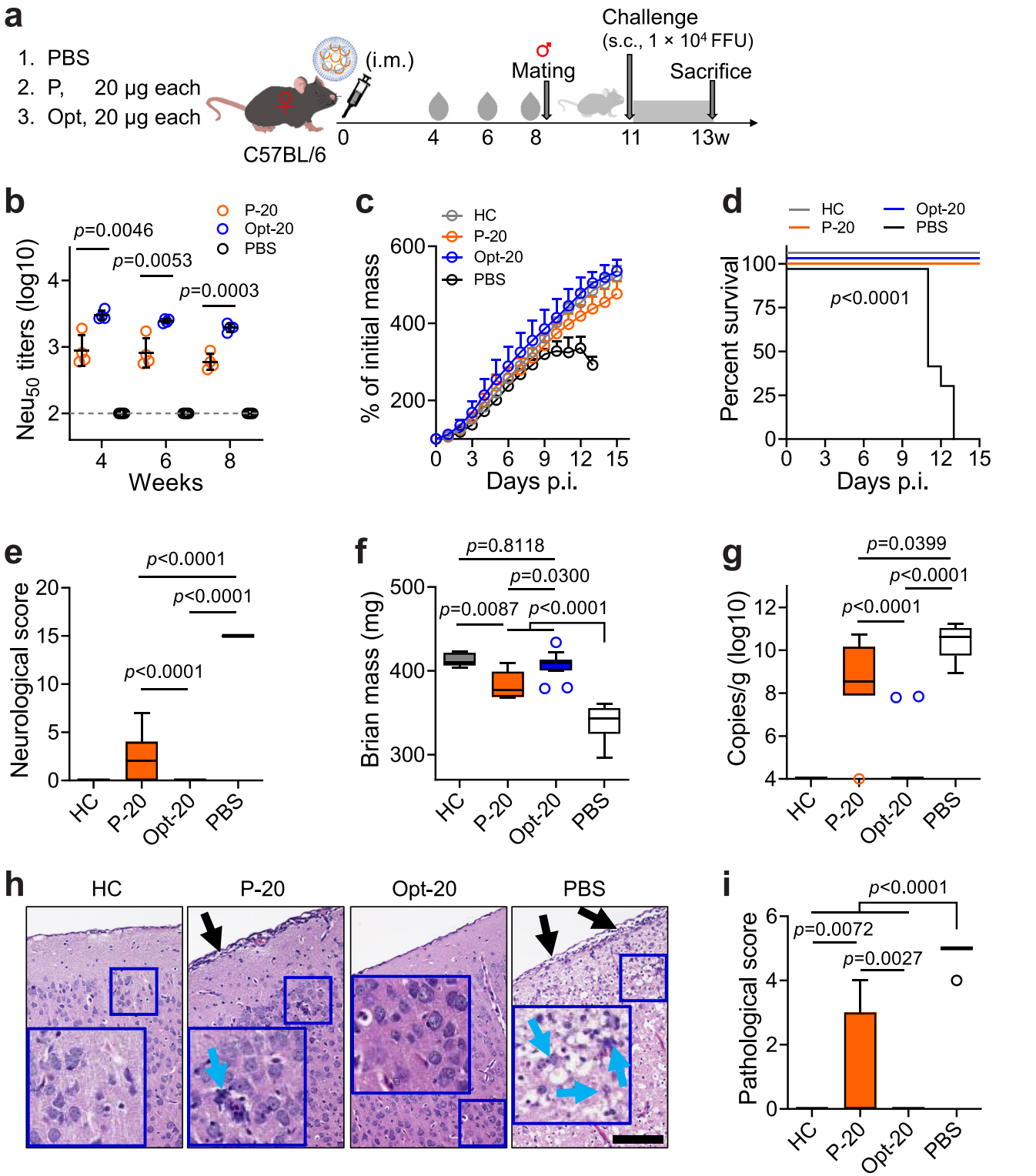

Fig. 7 | Durability of the protective immunity elicited by optimized EN(LNP) in mice. a Schematic diagram of immunization and challenge assay. Eight-week-old female C57BL/6 mice were i.m. immunized once with prototype (P) or optimized (Opt) EN(LNP) at the indicated doses. At 4, 6, and 8 weeks after immunization, mice sera were collected. At 8 weeks after immunization, immunized female mice were mated. After birth at 11 weeks, 1-day-old pups were s.c. challenged with 1×10^4 FFU of ZIKV. At 15 days after challenge, pups were sacrificed. **b** anti-ZIKV nAb titers at 4, 6, or 8 weeks after immunization. LOD is 100 and marked by gray dashed line. **c** Growth curves of the pups. **d** Survival curves of the pups. Comparisons were conducted between each group and HC. **e** Neurological scores of the pups at 15 days after challenge. **f** Brain masses of the pups at sacrifice. **g** ZIKV genome copies in neonatal brains at 15 days after challenge or at sacrifice. **h** H&E staining of brain tissue sections. Representative images are shown. Black arrows, meningeal lymphocyte infiltration. Cyan arrows, necrotic cells in cortex. Scale bar = 100 μm. **i** Pathological scores of neonatal brains. Box plots (**e**–**g**, **i**) indicate median (middle line), 25–75 percentile (box), 5–95 percentile (whiskers) and outliers (single points). Data points represent mean values of two technical replicates for one mouse (**b**) or mean values for one group (**c**). n = 4 for (**b**). n = 8 (HC), 7 (P-20), 13 (Opt-20) and 9 (PBS) for (**c**–**i**). Data are representative of two independent experiments and presented as mean ± s.d. Comparisons were performed by one-way ANOVA and Tukey's multiple comparison tests (**b**, **e**, **f**, **g**, **i**), or Log-rank (Mantel-Cox) tests (**d**). *p* values are shown on the graphs. Source data are provided as a Source Data file.

symptoms, and brain growth retardation (Fig. 7c–f). Prototype EN(LNP) also prevented mortality, but the pups experienced moderate growth delay and neurological disorders (Fig. 7c–f). In the optimized EN(LNP) group, 11 out of 13 pups showed no detectable viral genomes, a significant improvement over the prototype EN(LNP) group, wherein only 1 out of 7 pups had no detectable viral genomes (Fig. 7g). All pups in the optimized EN(LNP) group and 4 out of 7 pups in the prototype EN(LNP) group showed no signs of meningeal inflammation or cortical laminar necrosis (Fig. 7h, i). Optimized circRNA vaccine, therefore, elicits protective immunity lasting at least up to 11 weeks in mice.

circRNA optimization does not increase the risks of DENV2 ADE in mice

Finally, we determined whether optimized EN(LNP) caused any risks of DENV ADE. The immune sera of optimized EN(LNP), at either 2 or 8 weeks after immunization, showed higher anti-ZIKV IgG titers than those of prototype EN(LNP) (Fig. 8a, b). However, in both types of immune sera, the titers of anti-DENV IgG were comparable and low (Fig. 8a, b). Unlike ZIKV sera that enhanced DENV infection in K562 cells across a wide range of dilutions (1:100 to 1:62500), the optimized EN(LNP) sera showed mild ADE effects only at dilutions below 1:2500,

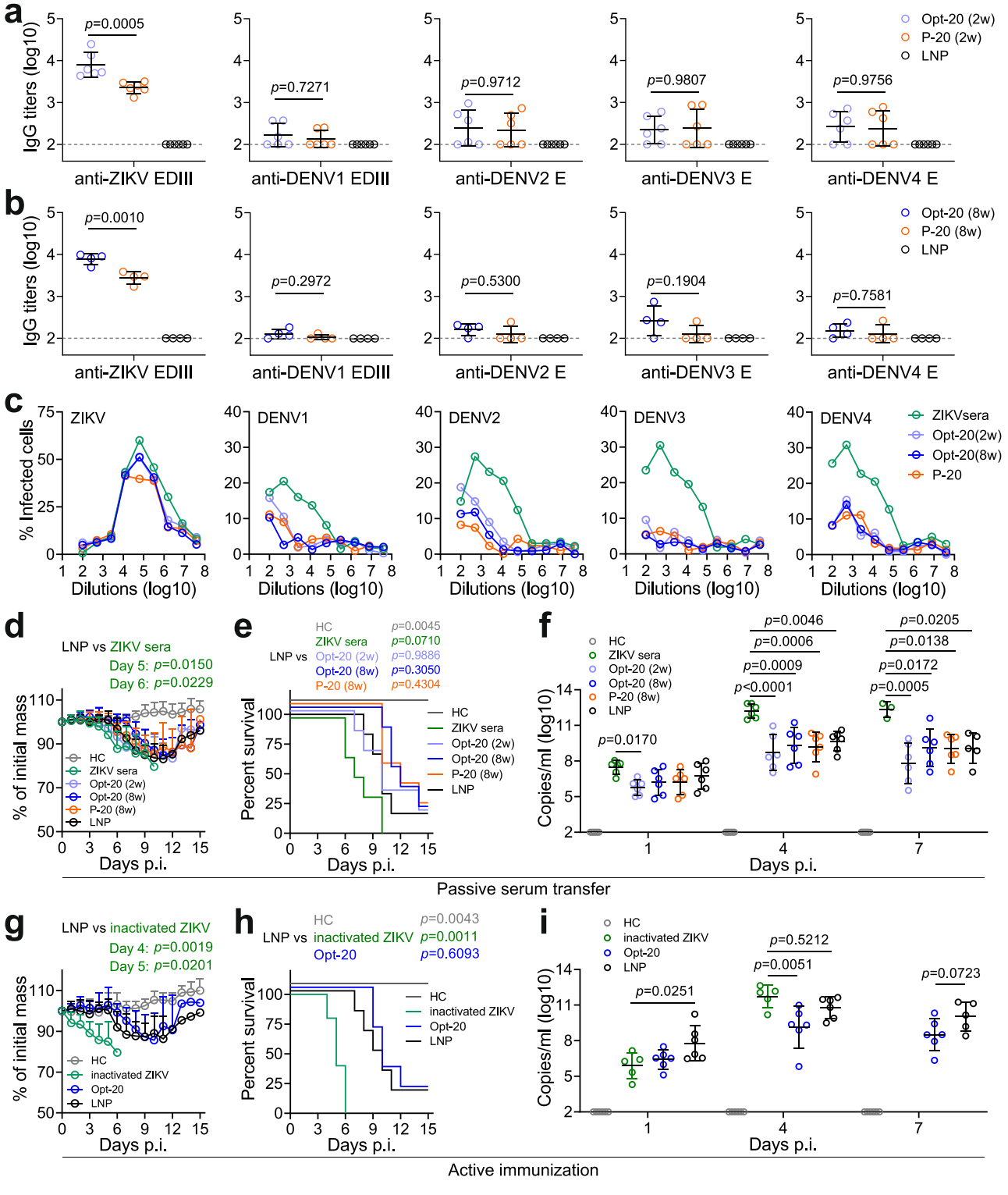

Fig. 8 | ADE risks of optimized EN(LNP) in mice. a, **b** Cross-reactivity of immune sera to ZIKV and DENV. Mice sera were collected at 2 (**a**) or 8 (**b**) weeks after immunization with the indicated vaccines. LODs are 100 and marked by gray dashed lines. **c** In vitro ADE activities of immune sera. Equally pooled mice sera in the indicated groups were 5-fold serially diluted (starting at 1:100) and incubated with ZIKV or DENV. The mixtures were used to infect K562 cells. Infected cells were examined by flow cytometry using mAb 8D10 (for ZIKV) or mAb ZK8-4 (for DENV). **d** Body masses of DENV2-infected *Ifnar*$^{-/-}$ mice that received immune sera before challenge. Equally pooled mice sera in each group were diluted tenfold with PBS. Twelve-week-old *Ifnar*$^{-/-}$ mice were i.p. inoculated with 200 µl of diluted sera 1 day before i.p. challenge with 1×10^6 FFU of mouse-adapted DENV2. **e** Survival curves. **f** DENV2 genome copies in the sera at 1, 4, and 7 days after challenge. **g** Body masses of DENV2-infected *Ifnar*$^{-/-}$ mice that received optimized EN(LNP) before challenge. Twelve-week-old *Ifnar*$^{-/-}$ mice were i.m. immunized with optimized EN(LNP), or empty LNPs, or 1×10^5 FFU of inactivated ZIKV (treated with 0.2% β-propiolactone and added with aluminum adjuvant) 3 weeks before challenge. **h** Survival curves. **i** DENV2 genome copies in the sera at 1, 4, and 7 days after challenge. Data points represent mean values of two (**a**, **b**) or three (**f**, **i**) technical replicates for one mouse, or mean values for one group (**c**, **d**, **g**). n = 6 for (**a**) and 4 for (**b**). n = 6 for (**d**–**f**). n = 5 (inactivated ZIKV) and 6 (HC, Opt-20, LNP) for (**g**–**i**). Data are representative of two independent experiments and presented as mean ± s.d. Comparisons were performed by one-way ANOVA and Tukey's multiple comparison tests (**a**, **b**, **d**, **g**, **f**, **i**), or by Log-rank (Mantel-Cox) tests between LNP group and the rest groups (**e**, **h**). *p* values are shown on the graphs. Source data are provided as a Source Data file.

although at the lowest dilution (1:100) the optimized EN(LNP) sera collected at 2 weeks showed comparable ADE effects on DENV1 and DENV2 infection as ZIKV sera (Fig. 8c). We adoptively transferred 200 µl tenfold diluted mice sera into *Ifnar*$^{-/-}$ mice 1 day before challenge with mouse-adapted DENV2. In contrast to ZIKV sera that aggravated the body mass loss, mortality, and viremia upon challenge, the optimized EN(LNP) sera, collected at either 2 or 8 weeks after immunization, showed no such aggravation, similar to the prototype EN(LNP) sera (Fig. 8d–f), suggesting that at the tested settings, the immune sera of optimized EN(LNP) unlikely promote DENV2 infection in mice.

We further assessed the ADE risks of active immunization with optimized EN(LNP). We i.m. immunized *Ifnar*$^{-/-}$ mice with optimized EN(LNP) (20 µg each circRNA) 3 weeks before i.p. challenge with mouse-adapted DENV2. Mice receiving empty LNPs or 1×10^5 FFU of inactivated ZIKV (treated with 0.2% β-propiolactone and added with aluminum adjuvant) served as controls. In contrast to ZIKV immunization that aggravated the body mass loss, mortality, and viremia upon challenge, immunization with optimized EN(LNP) showed no signs of DENV2 ADE, evidenced by the comparable body mass loss, mortality, and viremia as those observed in LNP-immunized mice (Fig. 8g–i). This result suggests that at the tested dose and timeframe, immunization with optimized EN(LNP) unlikely causes DENV2 ADE in mice.

Discussion

The overlapping endemic area and well-documented ADE between ZIKV and DENV necessitate a single-shot ZIKV vaccine offering rapid and durable protection without the risks of DENV ADE. We demonstrate that EDIII-Fc circRNA elicits robust anti-ZIKV nAbs but minimal DENV-reactive antibodies (Figs. 1, 5), and the combination of EDIII-Fc and NS1 circRNAs confers effective protection in two mouse models with no signs of DENV ADE (Figs. 3–8). Being one of the few single-shot vaccines tested so far[9], the circRNA vaccine offers advantages over live-attenuated vaccines, for which simultaneous protection against ZIKV and DENV might be desirable to avoid ADE[6,41]. Multivalent live-attenuated vaccines are prone to stimulate imbalanced immunity, sensitizing seronegative individuals to enhanced disease upon natural infection[6]. Dengvaxia, a tetravalent live-attenuated vaccine that increases the risks of severe dengue in DENV-naïve recipients[42], elicits DENV4-specific nAbs and cross-reactive nAbs against DENV1-3[43]. The cross-reactive nAbs may rapidly decline, leading to short-term protection but to risks of ADE thereafter. TAK003, another tetravalent live-attenuated DENV vaccine, elicits DENV2-biased immunity[44]. Subunit vaccines using engineered E or EDIII can trigger homotypic nAbs but typically require multiple doses to achieve full protection[15]. An adenovirus-vectored vaccine expressing engineered E proteins elicits ZIKV-specific and sterilizing immunity, albeit at a dose too high (1.6×10^{11} viral particles per mouse) to be clinically applicable[9]. Hence, our circRNA vaccine produces favorable results and deserves further evaluation.

Our data expand understanding about the immunological properties of circRNA vaccines. To date, only a few studies have explored circRNA vaccines against SARS-CoV-2, monkeypox, or tumor[30,45,46]. We found that LNP-delivered circRNAs induced the GC reactions and antibody responses of high quality (Fig. 1), which are critical for vaccines against ZIKV or DENV, because the nAb epitopes on E proteins are usually subdominant[14]. The EDIII-Fc circRNA also elicited robust Th1 and $CD8^+$ T cell responses (Fig. 1), as did the circRNA-based SARS-CoV-2 vaccines[30]. This may facilitate viral clearance in blood and central nerves system of the adult mouse model (Figs. 2 and 6)[47]. Moreover, we found that the translation efficiency of circRNA vaccines was crucial for the protective efficacy (Figs. 3, 4, 6). The removal of impurities, including excised introns and remnant precursors, elevated the translation level (Supplementary Fig. 1)[36]. Consistent with previous results[40], the employment of iHRV-B3 and proper UTRs elevated the translation level of EDIII-Fc and NS1 (Fig. 6). It has been shown that wild-type iHRV-B3 drives stronger translation than iCVB3[40]. The PABP-binding motif at the 5′ UTR, as well as the 3′ UTR of HBA1 mRNA, have been utilized in linear mRNA vaccines to enhance the stability and translation[48–50]. Our results, along with previous ones[40], illustrate the importance of such elements for circRNA vaccines, which may confer higher and prolonged translation of target antigens, enabling greater nAb responses and durable protection (Fig. 7). However, even in the presence of such elements, the translation of circRNAs reported here was not as high as their linear mRNA counterparts (Supplementary Fig. 10). This might be attributed to the inherently lower efficiency of cap-independent translation initiation in comparison with the cap-dependent pathway[51]. The secondary structure formed by the 3′ region of the IRES and the downstream coding sequence might also affect the translation strength[40]. Further optimization, such as introducing m^6A methylation, IRES trans-acting factors, or modifications in the coding sequence[40], is needed to improve the protective efficacy or reduce the dosage of circRNA vaccines.

Importantly, we demonstrate that the combination of EDIII-Fc and NS1 has the potential to provide full protection. Subunit vaccines based on genetic vectors usually employ prM/M to assist the folding of E in order to improve the nAb responses[7,39]. Without prM/M, both ADE-prone antibodies and nAbs may be reduced[39]. EDIII, in its native or a modified form, avoids inducing ADE-prone antibodies against prM/M, EDI or EDII[14,15], but the immunogenicity is limited[14,15]. The vaccine candidates using native EDIII alone are insufficient to protect against ZIKV infection[14]. EDIII-Fc circRNA, although elicited comparable maternal nAbs as EN(LNP) did (Figs. 1–4), did not prevent ZIKV infection without NS1 circRNA (Figs. 2–4), highlighting the importance of anti-NS1 antibodies[19–23]. Anti-E and anti-NS1 antibodies work together to inhibit the entry and dissemination of ZIKV in pups[20,39], since maternal antibodies but not lymphocytes can be vertically transferred and take effects[52]. It has been proposed that the limited protective efficacy of Dengvaxia is partially attributed to the lack of anti-NS1 antibodies[53]. Therefore, our results, along with previous studies[24],

provide insights for rational design of subunit vaccines against flavivirus infection.

We noted that EDIII-Fc circRNA elicited residual DENV-reactive antibodies in a proportion of animals (Figs. 5, 8), implying that EDIII contains some epitopes targeted by cross-reactive antibodies, consistent with previous observations that the ABDE-sheet of ZIKV EDIII and the AB loop of DENV EDIII were recognized by non- or less neutralizing antibodies[54,55]. These epitopes are unlikely dominant in the context of dimeric EDIII-Fc, as evidenced by the low titers and rapid decline of the DENV-reactive antibodies (Figs. 5, 8 and Supplementary Fig. 7). Although the immune sera promoted DENV infection moderately in cell cultures, they did not aggravate the infection or disease severity of DENV2 in mice (Figs. 5, 8), implying that under the tested conditions, the residual cross-reactive antibodies elicited by circRNA vaccines are insufficient to promote DENV2 infection in vivo. The results of active immunization studies also support this observation. Neither prototype nor optimized EN(LNP), eliciting different levels of antibody responses (Fig. 6j and Supplementary Fig. 11f), caused any signs of ADE of DENV2 infection in the immunized *Ifnar*$^{-/-}$ mice (Figs. 5, 8). However, caution should be exercised when generalizing the results of mouse models to human scenarios, because the pathogenesis of ADE in humans is complicated and has not been fully understood yet. The occurrence of ADE in humans involves multiple contributing factors, including afucosylation of IgG1, polymorphism of FcγRs, and aberrant innate immunity[56–59], which may be distinct to the pathogenesis of ADE in mice models. Further studies in non-human primates and clinical trials, therefore, are essential for comprehensively evaluating the risks of ADE associated with circRNA vaccines.

Although the maternal immunization and neonatal challenge model used in this study is less physiologically relevant to congenital Zika syndrome (CZS) in human compared to the preclinical pregnancy models used in other studies[60–62], it may represent a stringent model for evaluating the protective efficacy of maternal immunity. Unlike the pregnancy animal models wherein both nAbs and T cell responses contribute to restricting the inoculated ZIKV from crossing the placental barriers[61,63], in the challenged pups only the nAbs inherited from the dams can confer protection. In addition, it has been reported that in pregnant mice, the monocytes or macrophages in the placenta play significant roles in inhibiting ZIKV transmission to the fetus, another barrier absent in the challenged pups[64]. In this respect, our results support that EN(LNP), especially the optimized version, elicits protective immunity of high magnitude and quality, thereby conferring complete protection against ZIKV infection in this stringent model (Fig. 6).

In the adult *Ifnar*$^{-/-}$ mice model, both nAbs and anamnestic T cell responses, in particular the CD8$^+$ T cell responses, may contribute to the protection. Human CD8$^+$ T cell responses triggered by natural infection preferentially target the high conserved regions in non-structural proteins such as NS3 and NS5 but not E or NS1[65], raising the concern that an evaluation in this model may over-estimate the protective efficacy of EN(LNP). Actually, EDIII-Fc and NS1, encoded by EN(LNP), contain several epitopes restricted by human HLA class I. CD8$^+$ T cells specific for FSS-E$_{337–347}$ (in EDIII) and FSS/MR-NS1$_{99–107}$ (in NS1), restricted by human HLA-B*0702, could be detected in HLA-B*0702 transgenic mice infected by ZIKV. Similarly, CD8$^+$ T cells specific for FSS/MR-E$_{377–386}$ (in EDIII) and FSS/MR-NS1$_{23–31}$ (in NS1), restricted by human HLA-A*0101, could be detected in HLA-A*0101 transgenic mice infected by ZIKV[66]. This implies that EN(LNP) or the optimized version has the potential to trigger EDIII- or NS1-specific CD8$^+$ T cell responses in individuals carrying the HLA-A*0101 or HLA-B*0702 allele. The strength of human CD8$^+$ T cell response elicited by EDIII and NS1 might be distinct to that in mice, but the protective antibody responses can partially bridge the gap. Indeed, protective antibody responses, as long as they are high enough, are sufficient to prevent ZIKV infection in neonatal brains (Figs. 4, 6).

In summary, we developed a circRNA vaccine strategy based on EDIII-Fc and NS1, which effectively protected against ZIKV infection without any signs of DENV2 ADE in mice. Our results propose circRNA as a promising platform for a safe and effective flavivirus vaccine.

Methods

Cell lines

African green monkey kidney Vero cells (CCL-81), HEK293T cells (CRL-3216), and human lung cancer A549 cells (CCL-185) were purchased from American Type Culture Collection (ATCC) and cultured in Dulbecco's modified Eagle medium (DMEM) with 10% fetal bovine serum (FBS). Human chronic myelogenous leukemia K562 cells (CCL-243) were purchased from ATCC and cultured in RPMI 1640 with 10% FBS. Expi293F cells were purchased from Thermo Fisher Scientific (R79007) and cultured in Union 293 Cell Feed Medium (Union-Biotech) with 10% FBS. All cells were maintained at 37 °C in an atmosphere containing 5% CO_2.

Viruses

ZIKV strain GZ02 (GenBank No. KX056898.1) was isolated from a Chinese patient returning from Venezuela in 2016[67]. DENV1 strain Hawaii (GenBank No. EU848545.1), DENV2 strain 16681 (GenBank No. U87411.1), DENV3 strain D191267 (GenBank No. OQ948473.1), and DENV4 strain H241 (GenBank No. AY947539.1) have been described[20,68,69]. All viruses were propagated in Vero cells.

Mouse-adaptive DENV2 was established according to previously described methods[70]. In brief, 1-day-old C57BL/6 mice were s.c. inoculated with 1×10^4 FFU of DENV2. Three days later, the brains were harvested, homogenized and centrifuged, and the supernatants were used to infect Vero cells. Another three days later, viruses in the culture media were concentrated with Amicon Ultra-15 Centrifugal Filter Unit (100 kDa, Merck Millipore) and s.c. injected into 1-day-old C57BL/6 mice. After 3 alternative passages between Vero cells and the pups, the obtained virus was propagated in Vero cells. Genome sequence of mouse-adaptive DENV2 was analyzed by next-generation and Sanger sequencing (GeneBank No. PQ008452). All the virus stocks were titrated by focus-forming assays in Vero cells and stored at −80 °C.

Recombinant proteins

ZIKV EDIII and NS1 proteins were produced in *E.coli* and Expi293F cells respectively. In brief, the coding sequence of EDIII (residues 298 to 409 of E protein[71]) was optimized according to *E.coli* codon usage, synthesized, and cloned into pET28a with a 6 × His-tag sequence fused at the 5′ terminus. EDIII was expressed in *E.coli* BL21 (DE3) according to previously described methods[72], refolded, and purified by Ni-NTA affinity column chromatography. The coding sequence of NS1 was optimized according to mammalian codon usage, synthesized, and cloned into pVAX1 with a tPA signal sequence fused at the 5′ terminus. After transfection with pVAX1-NS1, the culture supernatants of Expi293F cells were harvested, and NS1 was purified by Ni-NTA affinity column chromatography. The proteins were verified by western blot analysis using human anti-EDIII monoclonal antibody (mAb) 8D10[73] and human anti-NS1 mAb 749-A4[22], respectively. Purified EDIII of DENV1 and E proteins of DENV2-4 were purchased from Sino Biological.

circRNA plasmids

Prototype circRNA vaccines were constructed based on the group I intron sequence of Anabaena pre-tRNA[36]. In brief, a fragment covering the following elements from 5′ to 3′ terminus was synthesized (Tsingke Biotechnology): 5′ homology arm, 3′ intron, an upstream spacer (5′-GGTAGTGGTGCTACTAACTTCAGCCTGC TGAAGCA-3′), iCVB3, a Kozak sequence (GCCACC), tPA sequence, a downstream spacer (5′-GGTAGTAAACTACTAACTACAACCTGCTGAAGCA-3′), 5′ intron, and 3′

homology arm. The fragment was cloned into pGEM-T-easy backbone (Promega, A1380) (Supplementary Fig. 1a).

Optimized circRNA vaccines were constructed using the group I intron sequence of the Td gene of T4 bacteriophage[40]. In brief, a fragment covering the following elements from 5′ to 3′ terminus was synthesized (Tsingke Biotechnology): 3′ intron, a 5′ UTR containing an RNA-binding motif of PABPv3 (AAAAAAAAAAAACCAAAAAAAA AAAACAAAAAAAAAAAATAATTGACTAA), iHRV-B3 with an Apt-eIF4G at the proximal loop of domain IV, a Kozak sequence, the tPA sequence, the 3′ UTR of HBA1, and 5′ intron. The fragment was also cloned into pGEM-T-easy backbone (Supplementary Fig. 9a).

The coding sequences of ZIKV EDIII (optimized according to mammalian codon usage), NS1 (optimized according to mammalian codon usage), EGFP, Gluc and Fluc were amplified by PCR and inserted just downstream of the tPA sequence in the pGEM-T-easy vectors mentioned above using ClonExpress II One Step Cloning Kit (Vazyme). To construct dimeric and trimeric EDIII, the coding sequence of human IgG1 Fc region was fused to the COOH terminus of EDIII to obtain EDIII-Fc, whereas the foldon motif of bacteriophage T4 fibritin protein was fused to the COOH terminus of EDIII with a 4 × GS linker to obtain EDIII-Fd.

Production of circRNAs

All the circRNAs were prepared according to previously described methods[36]. In brief, DNA templates for circRNA precursors or control linear precursors were amplified by PCR from their respective pGEM-T-easy plasmids. The primers used were as follows. For circRNA precursors, the universal forward, 5′-GCTTTAATACGACTCACTATAGGGG-3′; reverse for Anabaena intron, 5′-CTAGA TATGCTGTTATCCGTCGA-3′; reverse for T4 Td intron, 5′-CTGCAGGTCGACTC TAGAGAA-3′. For control linear precursors, the universal forward primer was the same as mentioned above; reverse for Anabaena intron, 5′-CTCGCCGGTAACGCAT AATAGCC-3′; reverse for T4 Td intron, 5′-GTCAGACTTTATTCAAAGACCACGG G-3′. Compared to circRNA precursors, the corresponding control linear precursors have the 5′ intron truncated and thus cannot be circularized. Program was set up as: 95 °C for 10 min; 30 cycles of 95 °C for 10 s, 60 °C for 10 s, and 72 °C for 10 s per kilo base pairs (kbp); 72 °C for 7 min. circRNA precursors and control linear precursors were produced using HiScribe T7 High Yield RNA Synthesis Kit (NEB, E2050S). Residual DNA templates were digested with DNase I (NEB, M0303S) at 37 °C for 15-30 min. Total RNAs were extracted using lithium chloride (LiCl, 7.5 M, Thermo Fisher Scientific, AM9480) and quantified using Nanodrop 8000. For circularization, 50 μg circRNA precursors were heated at 70 °C for 5 min and immediately chilled on ice for 5 min. GTP (Thermo Fisher Scientific, R0461) was added at a final concentration of 2 mM along with T4 RNA Ligase Reaction Buffer (containing 10 mM Mg^{2+}, NEB, B0216L) and incubated at 55 °C for 15 min. Finally, circRNAs were extracted by LiCl precipitation, dissolved in nuclease-free water, and subjected to HPLC purification.

RNase R digestion

In brief, 20 μg circRNA or control linear precursors were incubated at 65 °C for 3 min, chilled on ice for 3 min, and added with 20 U RNase R (Epicentre, RNR07250). After digestion at 37 °C for 30 min or 240 min (for NS1 circRNAs only), RNAs were extracted by LiCl precipitation and subjected to agarose-gel electrophoresis.

Junction site PCR

In brief, 10 μg circRNA was treated with RNase R and purified using the MEGAclear Transcription Clean-up kit (Thermo Fisher, AM1908). Control linear precursors were examined in parallel. cDNAs were synthesized using GoScript Reverse Transcription System (Promega, A5001) with random primers. Junction site PCR was carried out using primers as follows. For Anabaena intron junction site, forward, 5′-CAAAACGGCTATTATGCGTTACC-3′; reverse, 5′-ATACCAGAGTG CTAGCGCC-3′. For T4 Td intron, forward, 5′-TAAGCTG-GAGCCTCGGTG-3′; reverse, 5′-GTTCAGGAAGGGTACAATGGG-3′. Program was set up as: 95 °C for 10 min; 25 cycles of 95 °C for 10 s, 60 °C for 10 s, and 72 °C for 10 s; 72 °C for 1 min. PCR products were subjected to agarose-gel electrophoresis and Sanger sequencing.

HPLC purification

In brief, after LiCl precipitation, circRNA mixtures were loaded onto a 10 × 300 mm size exclusion column with particle size of 5 μm and pore size of 2000 Å (Sepax Technologies, 215980P-10030) and eluted with RNase-free TE buffer (pH = 8.0, Coolaber, SL2082) on an Agilent 1260 Series HPLC (Agilent) at a flow rate of 1.65 ml/min. Fractions were collected as indicated, quantified by measuring the absorption values at 260 nm, and subjected to agarose-gel electrophoresis. circRNAs were then enriched using Amicon Ultra-15 Centrifugal Filter (50 kDa, Merck Millipore) and dissolved in RNase-free water.

LNP encapsulation

circRNAs were encapsulated with LNPs according to previously described methods[74]. In brief, circRNA-LNPs were formulated by mixing the ethanol phase containing ionizable lipids (SINOPEG, SM102/DSPC/cholesterol/DMG-PEG 2000 at molar ratios of 50:10:38.5:1.5) with the aqueous phase containing circRNA in acetate buffer (pH = 5.0) at a ratio of 3:1 (lipids: RNA) on a microfluidic chip device (Micro & nano). circRNA-LNPs were then re-suspended in PBS (pH = 7.4) and filtered using Amicon Ultra-15 Centrifugal Filter (10 kDa, Merck Millipore). Encapsulation rates and circRNA concentrations were measured using the Quant-it RiboGreen RNA Assay Kit (Invitrogen, R11490). The size of circRNA-LNPs was measured using dynamic light scattering (Malvern Zetasizer) and analyzed using Zetasizer software.

circRNA transfection assay

In brief, HEK293T or A549 cells were transfected with each circRNA (for 24-well plates: 2, 1, 0.5 or 0.2 μg per well; for 96-well plates: 200, 100, or 50 ng per well) using Lipofectamine MessengerMax (Invitrogen, LMRNA003), following the manufacturer's instructions. To test the expression of EDIII or NS1, cell lysates and culture media were harvested at 24 or 48 h after transfection and subjected to western blot analysis. To test the expression of EGFP, A549 cells were observed under a fluorescence microscope (Olympus) and images were captured at 48 h after transfection. The Fluc in cell lysates and Gluc in culture media were tested at 24 h after transfection using Luciferase Assay System (Promega) or coelenterazine (Coolaber), respectively. RLUs were recorded by GloMax Discover Microplate Reader (Promega).

Western blot analysis

In brief, cell lysates or culture media were added with loading buffer in the presence or absence of β-mercaptoethanol. Proteins were separated by SDS-PAGE and transferred onto nitrocellulose membrane (GE Healthcare). After blocked with 5 % skimmed milk in PBS containing 0.05% Tween 20 (PBST) at 37 °C for 1 h, membranes were incubated with anti-ZIKV E mAb 8D10, anti-ZIKV NS1 mAb 749-A4, EDIII protein immune mice sera, or mouse anti-GAPDH antibody (Beyotime) at 4 °C overnight. After thoroughly washed with PBST, membranes were incubated with HRP-conjugated goat anti-human or anti-mouse IgG antibodies for 1 h (Beyotime) and developed with chemiluminescent substrates (GeneStar). Protein signals were captured by chemiluminescent Western blot imaging system (Biorad).

Animals

Eight-week-old C57BL/6 mice and CD-1(ICR) mice were purchased from GemPharmatech Co., Ltd. *Ifnar*$^{-/-}$ C57BL/6 mice were constructed by CRISPR-Cas9 technology at Cyagen Biosciences. All animals were

bred and housed in the Animal Experimental Center of Guangzhou Institutes of Biomedicine and Health (GIBH). Mice were housed in an SPF barrier facility with 12 h/12 h light/dark cycles, a temperature of 20–23 °C, and humidity of 50-60%. Challenge assays involving ZIKV or DENV were conducted under animal biosafety level 2 (ABSL-2) plus conditions. All experiment protocols were approved by the Institutional Animal Care and Use Committee of GIBH (IACUC, No. 2021061).

Immunization and challenge assays

To test the immunogenicity of EDIII, EDIII-Fc or EDIII-Fd circRNA (Figs. 1, 2), 8-week-old C57BL/6 mice (female), or 12-week-old *Ifnar*$^{-/-}$ C57BL/6 mice (male and female) were i.m. immunized once or twice (at a 3-week-interval) with circRNA-LNP (containing 20 μg circRNA per mouse) in 200 μl PBS. Control mice received an equal mass of empty LNPs or equal volume of PBS. Sera, spleens, or inguinal lymph nodes were harvested at the indicated time points and subjected to antibody or lymphocyte examination.

To test the immunogenicity of prototype and optimized EN(LNP) (Figs. 3, 4, 6), 8-week-old C57BL/6 mice (female) or 12-week-old *Ifnar*$^{-/-}$ C57BL/6 mice (male and female) were i.m. immunized once or twice (at a 3-week interval) with EN(LNP), EN(RNA), EDIII-Fc circRNA, NS1 circRNA, optimized EN(LNP), or the m1Ψ-modified mRNAs at 5 or 20 μg each RNA as indicated. Sera or inguinal lymph nodes were collected and subjected to antibody or lymphocyte examination.

To test the protective effects of circRNA vaccines, two models were used. For the maternal immunization and neonatal challenge model, immunized female C57BL/6 mice were mated with unimmunized male mice at 2 (Figs. 2–4), 3 (Fig. 6), or 8 (Fig. 7) weeks after the final immunization. After birth, 1-day-old pups were s.c. injected with 1×10^4 FFU of ZIKV in 50 μl PBS. HC pups received 50 μl PBS via the same route. Body masses and symptoms were recorded daily. Pups that showed continuous loss of body mass for two days were considered dead and euthanized. At 15 days after challenge, neurological scores, mainly the paralysis of limbs and tail, were recorded in a single-blind manner. Pups were sacrificed and brain tissues were harvested and subjected to viral load detection or histological analysis.

For the adult *Ifnar*$^{-/-}$ C57BL/6 mice model, immunized mice (male and female) were s.c. challenged with 1×10^5 FFU of ZIKV in 100 μl PBS at 12 days (Supplementary Fig. 6) or 3 weeks (Figs. 2 and 6) after the final immunization. HC mice received 100 μl PBS via the same route. Body masses were recorded daily. Mice that had lost 20% of initial body mass were considered dead and euthanized. Sera were collected at 1, 4, and 7 days after challenge. At 10 or 15 days after challenge, mice were sacrificed. Sera, brains, and spleens were harvested and subjected to viral load detection.

To test the virulence of mouse-adapted DENV2 in mice, 1-day-old CD-1(ICR) mice were intracerebrally challenged with 1×10^4 FFU of parental or mouse-adapted DENV2. Body masses and symptoms were recorded daily.

Enzyme-linked immunosorbent assay (ELISA)

In brief, 96-well ELISA plates were coated with purified ZIKV EDIII, DENV1 EDIII, E proteins of DENV2-4, or ZIKV NS1 at 50 ng per well at 4 °C overnight. After washed 3 times with PBST, plates were blocked with PBST containing 5% skimmed milk at 37 °C for 1 h. Mice sera were 4-fold serially diluted (starting from 1:100 or as indicated), added to each well, and incubated at 37 °C for 2 h. LNP- or PBS-immunized mice sera were used as negative controls. After washed 3 times with PBST, plates were added with an HRP-conjugated goat anti-mouse IgG antibody (Beyotime), incubated at 37 °C for 1 h, and washed 5 times with PBST. The reactions were developed with 100 μl TMB/E substrates (Merck Milipore) and terminated with 2 M H_2SO_4. Finally, OD450 values were recorded by Microplate Reader Epoch2 (BioTek). IgG titers were calculated as the reciprocals of the maximal dilutions at which the OD450 values were equal to or higher than the cut-off values (2.1 times that of the negative control wells).

Flow cytometry-based neutralization test (FNT)

FNT was performed according to previously reported methods[39]. In brief, Vero cells were seeded into 96-well plates at 2×10^4 cells per well and cultured overnight. Mice sera were 4-fold serially diluted in DMEM (starting from 1:50 or 1:100) and incubated with ZIKV (200 FFU per well) at 37 °C for 1 h. LNP- or PBS-immunized mice sera were used as negative controls. The mixtures were added onto cells, incubated at 37 °C for 2 h, and replaced with fresh DMEM containing 2% FBS. Three days later, cells were fixed and permeabilized with Cytofix/Cytoperm buffer (BD). Cells were then labeled with mAb 8D10, stained with an Alexa Fluor 647-conjugated goat anti-human IgG antibody (SouthernBiotech, 2040-31), and analyzed on Accuri C6 flow cytometer (BD). Half-maximal neutralizing antibody (Neu_{50}) titers were calculated as the dilutions at which the E-positive cells were reduced by 50% relative to negative controls.

Flow cytometry of Tfh, GC B and plasma cells

In brief, lymphocytes were isolated from the ILNs by passing through 200-mesh stainless steel wire meshes. Cells were blocked with an Fc receptor antibody α-CD16/32 (clone: 2.4G2) on ice for 5 min, followed by staining with fluorochrome-conjugated antibodies in PBS with 2% FBS: for the Tfh cell panel, CD3 (PerCP/Cy5.5, clone: 17A2, BioLegend), CD4 (APC, clone: RM4-5, BD), CXCR5 (PE, clone: 2G8, BD), PD-1 (BV421, clone: EH12.1, BD); for the GC B cell and plasma cell panels, CD45R (PE/Cy7, clone: RA3-6B2, BD), CD38 (PerCP/Cy5.5, clone: 90/CD38, BD), CD138 (PE, clone: 281-2; BD), CD95 (BV421, clone: Jo2, BD), GL7 (Alexa Fluor 647, clone: GL7, BD). The staining was performed on ice for 30 min. Finally, cells were fixed and analyzed by LSRFortessa (BD).

Intracellular cytokine staining (ICS) assay

In brief, lymphocytes were isolated from the spleens by passing through 200-mesh stainless steel wire meshes followed by density gradient centrifugation using mouse lymphoid separation medium (Dakewe). Cells were seeded into 96-well plates (2×10^6 cells per well) and stimulated with overlapping peptide pools (2 μg/ml of each peptide) corresponding to ZIKV E protein. Unstimulated cells were used as controls. After incubated at 37 °C for 2 h, cell cultures were added with brefeldin A (10 mg/ml; BD) and incubated at 37 °C for another 10 h. After washed twice with PBS, cells were blocked with mAb α-CD16/32 on ice for 5 min and stained with the following surface marker antibodies in PBS (containing 2% FBS) on ice for 30 min: CD3 (BV421, clone: 17A2, BioLegend), CD4 (APC, clone: RM4-5, BD), and CD8α (FITC, clone: 53-6.7, BioLegend). Cells were then fixed and permeabilized with Cytofix/Cytoperm buffer at 4 °C for 30 min. Finally, cells were stained with intracellular antibodies against IFNγ (PE, clone: XMG1.2, BD), TNFα (APC/Cy7, clone: MP6-XT22, BioLegend) and IL-2 (BV605, clone: JES6-5H4, BioLegend) and analyzed on LSRFortessa.

Neurological scoring

On day 15 after challenge, neurological symptoms of the pups were scored in a single-blind manner[39]. Scores of each limb were designated as: 0, no sign; 1, weakness or altered gait; 2, paresis; 3, full paralysis. Scores of the tail were designated as: 0, no sign; 1, half paralysis; 2, full paralysis. The score of one pup was the sum of the scores from four limbs and the tail. Accordingly, the maximal score of a survival pup is 14. A pup that succumbed to infection received a score of 15.

Histological analysis

In brief, brain tissues were fixed in 10% neutral buffered formalin for 7 days and transferred to 70% ethanol. Subsequently, brain tissues were dehydrated via a serial ethanol gradient and embedded in paraffin wax blocks. Tissue sections (5-mm-thick) were prepared, dewaxed

in xylene, rehydrated via decreasing concentrations of ethanol, and washed with PBS. Tissue sections were then stained with hematoxylin for 8 min and eosin for 3 min. Finally, tissue sections were successively incubated with 70% ethanol for 20 s, 90% ethanol for 20 s, 100% ethanol for 1 min, and xylene for 3 min. Images were captured using TissueFAXS (TissueGnostics). The meningeal inflammation and cortex laminar necrosis were assessed in a single-blind manner. In brief, five versions in cerebral cortex were randomly selected for each section and scored. Scores of meningeal inflammation were designated as: 0, no lymphocyte infiltration; 1, mild lymphocyte infiltration; 2, moderate lymphocyte infiltration; 3, severe lymphocyte infiltration. Scores of cortex laminar necrosis were designated as: 0, no signs of necrosis; 1, mild necrosis; 2, moderate to severe necrosis. Accordingly, the maximal pathological score of one version is 5. The median score of the 5 versions were designated as the score of that mice.

Quantitative real time PCR (qRT-PCR)

Genome copy numbers of ZIKV or DENV2 in the sera or tissues were measured using qRT-PCR as described previously[39,75]. In brief, total RNAs were extracted using TRIzol (Thermo Fisher Scientific). qRT-PCR was carried out using HiScript II One Step qRT-PCR SYBR Green Kit (Vazyme). The primers used were as follows. For ZIKV, forward, 5′-TGGAGGCTGAGGAAGTTCTA G-3′; reverse, 5′-CTTCA-CAACGCAATCATCTCCACTG-3′. For DENV2, forward, 5′-CAGGT-TATGGCACTGTCACGAT-3′; reverse, 5′-CCATCTGCAGCAACACCAT CTC-3′. Program was set up as: 50 °C for 30 min; 95 °C for 10 min; 45 cycles of 95 °C for 30 s, 60 °C for 30 s, and 72 °C for 30 s. Melting curves were produced at 65 °C to 95 °C with an increment of 0.5 °C per cycle for 5 s. Standard curves were created using ZIKV RNAs corresponding to NS5 or DENV2 RNAs corresponding to E, which were generated by IVT. Viral loads were calculated as genome copy numbers per gram tissues or per ml sera. LODs were about 1×10^4 copies per gram tissues or 1×10^2 copies per ml sera.

In vitro ADE assay

ADE effects of immune sera in cell cultures were measured using a flow cytometry-based assay[20]. In brief, mice sera were 5-fold serially diluted (starting from 1:100), mixed with ZIKV or DENV3 (1 FFU per cell), or with DENV1, DENV2, or DENV4 (0.2 FFU per cell) in RPMI 1640, and incubated at 37 °C for 1 h. C57BL/6 mice sera collected 2 weeks after ZIKV infection (1×10^5 FFU, s.c.) were also tested. The mixtures were added to K562 cells in 96-well plates and incubated at 37 °C for 2 days. Cells were fixed and permeabilized using Cytofix/Cytoperm buffer, and labeled with anti-ZIKV mAb 8D10, or with mAb ZK8-4 which was isolated from a ZIKV-infected patient and showed cross-reactivity to DENV E proteins[76]. Finally, cells were stained with an Alexa Fluor 647-conjugated goat anti-human IgG antibody (SouthernBiotech, 2040-31) and analyzed using Accuri C6 flow cytometer.

In vivo ADE assay

For the passive transfer model, the immune sera collected at 2 or 8 weeks after the final immunization were equally pooled for each group, inactivated by incubation at 56 °C for 30 min, and diluted ten-fold with PBS. Twelve-week-old *Ifnar*$^{-/-}$ C57BL/6 mice (male and female) were i.p. administrated with 200 µl diluted sera (equal to 20 µl pooled sera). One day later, mice were i.p. challenged with 1×10^6 FFU of mouse-adapted DENV2. The body masses and survival rates were monitored daily. Sera were collected at 1, 4, and 7 days after challenge and DENV2 genomes were measured by qRT-PCR. Mice that lost 20% of initial body mass were considered dead and euthanized.

For the active immunization model, 12-week-old *Ifnar*$^{-/-}$ C57BL/6 mice (male and female) were i.m. immunized with prototype or optimized EN(LNP) at 20 µg each circRNA per mouse, or 1×10^5 FFU of ZIKV which had been inactivated with 0.2% β-propiolactone and added with aluminum adjuvant, or an equivalent mass of empty LNPs. Mice receiving 200 µl diluted ZIKV sera 1 day before challenge were also used as controls. At 2 (Fig. 5f) or 3 (Fig. 8g–i) weeks after immunization, mice were challenged with 1×10^6 FFU of mouse-adapted DENV2. The survival, body masses, and serum viral loads were monitored or tested similarly.

Data process and statistics

Flow cytometry data were analyzed using FlowJo software v10 (BD). Comparisons between two groups were conducted by paired or unpaired, two-tailed Student's t-test. Comparisons among more than two groups were conducted by one-way ANOVA and Tukey's multiple comparison tests. Comparisons of the survival data were conducted by Log-rank (Mantel-Cox) tests. Statistical analyses were computed by GraphPad Prism 8 (GraphPad) and the details have been provided in each figure's legend. A p-value < 0.05 was considered statistically significant. Data graphs were constructed using GraphPad Prism 8. Figures were created using Adobe Illustrator 2021 (Adobe Systems Inc.) and PowerPoint 2013 (Microsoft).

Reporting summary

Further information on research design is available in the Nature Portfolio Reporting Summary linked to this article.

Data availability

The data supporting the findings of this study are available within the paper (and its supplementary information files). Source data are provided with this paper.

References

1. Pierson, T. C. & Diamond, M. S. The emergence of Zika virus and its new clinical syndromes. *Nature* **560**, 573–581 (2018).
2. https://www.who.int/publications/m/item/zika-epidemiology-update-may-2024.
3. Musso, D., Ko, A. I. & Baud, D. Zika Virus Infection - After the Pandemic. *N. Engl. J. Med.* **381**, 1444–1457 (2019).
4. Silva, N. M., Santos, N. C. & Martins, I. C. Dengue and Zika Viruses: Epidemiological History, Potential Therapies, and Promising Vaccines. *Tropic.medicine and infectious disease* **5**, https://doi.org/10.3390/tropicalmed5040150 (2020).
5. Fowler, A. M. et al. Maternally acquired zika antibodies enhance dengue disease severity in mice. *Cell Host Microbe* **24**, 743–750.e745 (2018).
6. Katzelnick, L. C. et al. Zika virus infection enhances future risk of severe dengue disease. *Science* **369**, 1123–1128 (2020).
7. Shukla, R., Ramasamy, V., Shanmugam, R. K., Ahuja, R. & Khanna, N. Antibody-dependent enhancement: a challenge for developing a safe dengue vaccine. *Front Cell Infect. Microbiol* **10**, 572681 (2020).
8. Richner, J. M. et al. Modified mRNA vaccines protect against zika virus infection. *Cell* **169**, 176 (2017).
9. Dai, L. et al. Protective Zika vaccines engineered to eliminate enhancement of dengue infection via immunodominance switch. *Nat. Immunol.* **22**, 958–968 (2021).
10. Metz, S. W. et al. Oligomeric state of the ZIKV E protein defines protective immune responses. *Nat. Commun.* **10**, 4606 (2019).
11. Slon-Campos, J. L. et al. A protective Zika virus E-dimer-based subunit vaccine engineered to abrogate antibody-dependent enhancement of dengue infection. *Nat. Immunol.* **20**, 1291–1298 (2019).
12. Stettler, K. et al. Specificity, cross-reactivity, and function of antibodies elicited by Zika virus infection. *Science* **353**, 823–826 (2016).
13. Sapparapu, G. et al. Neutralizing human antibodies prevent Zika virus replication and fetal disease in mice. *Nature* **540**, 443–447 (2016).
14. Lopez-Camacho, C. et al. Immunogenicity and efficacy of zika virus envelope domain iii in dna, protein, and chadox1 adenoviral-

vectored vaccines. *Vaccines (Basel)* **8**, https://doi.org/10.3390/vaccines8020307 (2020).
15. Rong, H. et al. Self-assembling nanovaccine confers complete protection against zika virus without causing antibody-dependent enhancement. *Front. Immunol.* **13**, 905431 (2022).
16. Carpio, K. L. & Barrett, A. D. T. Flavivirus NS1 and Its Potential in Vaccine Development. *Vaccines* **9**, https://doi.org/10.3390/vaccines9060622 (2021).
17. Sun, J., Du, S., Zheng, Z., Cheng, G. & Jin, X. Defeat dengue and zika viruses with a one-two punch of vaccine and vector blockade. *Front. Microbiol.* **11**, 362 (2020).
18. Puerta-Guardo, H. et al. Flavivirus NS1 triggers tissue-specific vascular endothelial dysfunction reflecting disease tropism. *Cell Rep.* **26**, 1598–1613 e1598 (2019).
19. Biering, S. B. et al. Structural basis for antibody inhibition of flavivirus NS1-triggered endothelial dysfunction. *Science* **371**, 194–200 (2021).
20. Yu, L. et al. Monoclonal antibodies against zika virus ns1 protein confer protection via fcgamma receptor-dependent and -independent pathways. *Mbio* **12**, https://doi.org/10.1128/mBio.03179-20 (2021).
21. Modhiran, N. et al. A broadly protective antibody that targets the flavivirus NS1 protein. *Science* **371**, 190–194 (2021).
22. Wessel, A. W. et al. Antibodies targeting epitopes on the cell-surface form of NS1 protect against Zika virus infection during pregnancy. *Nat. Commun.* **11**, 5278 (2020).
23. Bailey, M. J. et al. Human antibodies targeting Zika virus NS1 provide protection against disease in a mouse model. *Nat. Commun.* **9**, 4560 (2018).
24. Bailey, M. J. et al. Antibodies Elicited by an NS1-Based Vaccine Protect Mice against Zika Virus. *Mbio* **10**, https://doi.org/10.1128/mBio.02861-18 (2019).
25. Grubor-Bauk, B. et al. NS1 DNA vaccination protects against Zika infection through T cell-mediated immunity in immunocompetent mice. *Sci. Adv.* **5**, eaax2388 (2019).
26. Brault, A. C. et al. A zika vaccine targeting ns1 protein protects immunocompetent adult mice in a lethal challenge model. *Sci. Rep.* **7**, 14769 (2017).
27. Kurup, D. et al. Measles-based Zika vaccine induces long-term immunity and requires NS1 antibodies to protect the female reproductive tract. *NPJ Vaccines* **7**, 43 (2022).
28. Dolgin, E. Why rings of RNA could be the next blockbuster drug. *Nature* **622**, 22–24 (2023).
29. Niu, D., Wu, Y. & Lian, J. Circular RNA vaccine in disease prevention and treatment. *Signal Transduct. Target Ther.* **8**, 341 (2023).
30. Qu, L. et al. Circular RNA vaccines against SARS-CoV-2 and emerging variants. *Cell* **185**, 1728–1744 e1716 (2022).
31. Hinke, D. M. et al. Antigen bivalency of antigen-presenting cell-targeted vaccines increases B cell responses. *Cell Rep.* **39**, 110901 (2022).
32. Suzuki, T. et al. Importance of neonatal FcR in regulating the serum half-life of therapeutic proteins containing the Fc domain of human IgG1: a comparative study of the affinity of monoclonal antibodies and Fc-fusion proteins to human neonatal FcR. *J. Immunol.* **184**, 1968–1976 (2010).
33. Junker, F., Gordon, J. & Qureshi, O. Fc gamma receptors and their role in antigen uptake, presentation, and t cell activation. *Front Immunol.* **11**, 1393 (2020).
34. Kim, M. Y., Mason, H. S., Ma, J. K. C. & Reljic, R. Recombinant immune complexes as vaccines against infectious diseases. *Trends Biotechnol.* https://doi.org/10.1016/j.tibtech.2024.05.004 (2024).
35. Yang, X. et al. Highly stable trimers formed by human immunodeficiency virus type 1 envelope glycoproteins fused with the trimeric motif of T4 bacteriophage fibritin. *J. Virol.* **76**, 4634–4642 (2002).
36. Wesselhoeft, R. A., Kowalski, P. S. & Anderson, D. G. Engineering circular RNA for potent and stable translation in eukaryotic cells. *Nat. Commun.* **9**, 2629 (2018).
37. De Silva, N. S. & Klein, U. Dynamics of B cells in germinal centres. *Nat. Rev. Immunol.* **15**, 137–148 (2015).
38. Laidlaw, B. J., Craft, J. E. & Kaech, S. M. The multifaceted role of CD4(+) T cells in CD8(+) T cell memory. *Nat. Rev. Immunol.* **16**, 102–111 (2016).
39. Liu, X. et al. Incorporation of NS1 and prM/M are important to confer effective protection of adenovirus-vectored Zika virus vaccine carrying E protein. *NPJ Vaccines* **3**, 29 (2018).
40. Chen, R. et al. Engineering circular RNA for enhanced protein production. *Nat. Biotechnol.* **41**, 262–272 (2023).
41. Shukla, R. et al. Dengue and Zika virus infections are enhanced by live attenuated dengue vaccine but not by recombinant DSV4 vaccine candidate in mouse models. *EBioMedicine* **60**, 102991 (2020).
42. Hadinegoro, S. R. et al. Efficacy and long-term safety of a dengue vaccine in regions of endemic disease. *N. Engl. J. Med* **373**, 1195–1206 (2015).
43. Henein, S. et al. Dissecting antibodies induced by a chimeric yellow fever-dengue, live-attenuated, tetravalent dengue vaccine (cyd-tdv) in naive and dengue-exposed individuals. *J. Infect. Dis.* **215**, 351–358 (2017).
44. White, L. J. et al. Defining levels of dengue virus serotype-specific neutralizing antibodies induced by a live attenuated tetravalent dengue vaccine (TAK-003). *PLoS neglected tropical Dis.* **15**, e0009258 (2021).
45. Zhou, J. et al. Circular RNA vaccines against monkeypox virus provide potent protection against vaccinia virus infection in mice. *Mol. Ther.* **32**, 1779–1789 (2024).
46. Li, H. et al. Circular RNA cancer vaccines drive immunity in hard-to-treat malignancies. *Theranostics* **12**, 6422–6436 (2022).
47. Lima, N. S., Rolland, M., Modjarrad, K. & Trautmann, L. T cell immunity and zika virus vaccine development. *Trends Immunol.* **38**, 594–605 (2017).
48. Kim, S. C. et al. Modifications of mRNA vaccine structural elements for improving mRNA stability and translation efficiency. *Mol. Cell Toxicol.* **18**, 1–8 (2022).
49. Xia, X. Detailed Dissection and Critical Evaluation of the Pfizer/BioNTech and Moderna mRNA Vaccines. *Vaccines (Basel)* **9**, https://doi.org/10.3390/vaccines9070734 (2021).
50. Zarghampoor, F., Azarpira, N., Khatami, S. R., Behzad-Behbahani, A. & Foroughmand, A. M. Improved translation efficiency of therapeutic mRNA. *Gene* **707**, 231–238 (2019).
51. Deviatkin, A. A. et al. Cap-independent circular mrna translation efficiency. *Vaccines (Basel)* **11**, https://doi.org/10.3390/vaccines11020238 (2023).
52. Kollmann, T. R., Marchant, A. & Way, S. S. Vaccination strategies to enhance immunity in neonates. *Science* **368**, 612–615 (2020).
53. Thomas, S. J. Is new dengue vaccine efficacy data a relief or cause for concern? *NPJ vaccines* **8**, 55 (2023).
54. Georgiev, G. I. et al. Resurfaced ZIKV EDIII nanoparticle immunogens elicit neutralizing and protective responses in vivo. *Cell Chem. Biol.* **29**, 811–823 e817 (2022).
55. Li, X. Q. et al. Dengue virus envelope domain III immunization elicits predominantly cross-reactive, poorly neutralizing antibodies localized to the AB loop: implications for dengue vaccine design. *J. Gen. Virol.* **94**, 2191–2201 (2013).
56. Bournazos, S. et al. Antibody fucosylation predicts disease severity in secondary dengue infection. *Science* **372**, 1102–1105 (2021).
57. Larsen, M. D. *et al*. Afucosylated IgG characterizes enveloped viral responses and correlates with COVID-19 severity. *Science* **371**, https://doi.org/10.1126/science.abc8378 (2021).

58. Bournazos, S., Gupta, A. & Ravetch, J. V. The role of IgG Fc receptors in antibody-dependent enhancement. *Nat. Rev. Immunol.* **20**, 633–643 (2020).
59. Narayan, R. & Tripathi, S. Intrinsic ADE: The Dark Side of Antibody Dependent Enhancement During Dengue Infection. *Front Cell Infect. Microbiol* **10**, 580096 (2020).
60. Kim, I. J. et al. Efficacy of an inactivated Zika vaccine against virus infection during pregnancy in mice and marmosets. *NPJ Vaccines* **7**, 9 (2022).
61. Kim, I. J. et al. Protective efficacy of a Zika purified inactivated virus vaccine candidate during pregnancy in marmosets. *NPJ Vaccines* **9**, 35 (2024).
62. Kim, I. J. et al. Zika purified inactivated virus (ZPIV) vaccine reduced vertical transmission in pregnant immunocompetent mice. *NPJ Vaccines* **9**, 32 (2024).
63. Elong Ngono, A. et al. CD8(+) T cells mediate protection against Zika virus induced by an NS3-based vaccine. *Sci. Adv.* **6**, https://doi.org/10.1126/sciadv.abb2154 (2020).
64. Winkler, C. W., Evans, A. B., Carmody, A. B. & Peterson, K. E. Placental Myeloid Cells Protect against Zika Virus Vertical Transmission in a Rag1-Deficient Mouse Model. *J. Immunol.* **205**, 143–152 (2020).
65. Rivino, L. et al. Differential targeting of viral components by CD4+ versus CD8+ T lymphocytes in dengue virus infection. *J. Virol.* **87**, 2693–2706 (2013).
66. Wen, J. et al. Identification of Zika virus epitopes reveals immunodominant and protective roles for dengue virus cross-reactive CD8(+) T cells. *Nat. Microbiol* **2**, 17036 (2017).
67. Zhang, S. et al. Chloroquine inhibits endosomal viral RNA release and autophagy-dependent viral replication and effectively prevents maternal to fetal transmission of Zika virus. *Antivir. Res.* **169**, 104547 (2019).
68. Hu, M. et al. Identification of an arylnaphthalene lignan derivative as an inhibitor against dengue virus serotypes 1 to 4 (denv-1 to -4) using a newly developed denv-3 infectious clone and replicon. *Microbiol Spectr.* **11**, e0042323 (2023).
69. Hao, J. et al. NLRC5 restricts dengue virus infection by promoting the autophagic degradation of viral NS3 through E3 ligase CUL2 (cullin 2). *Autophagy* **19**, 1332–1347 (2023).
70. Orozco, S. et al. Characterization of a model of lethal dengue virus 2 infection in C57BL/6 mice deficient in the alpha/beta interferon receptor. *J. Gen. Virol.* **93**, 2152–2157 (2012).
71. Tai, W. et al. Critical neutralizing fragment of Zika virus EDIII elicits cross-neutralization and protection against divergent Zika viruses. *Emerg. microbes Infect.* **7**, 7 (2018).
72. Viranaicken, W. et al. ClearColi BL21(DE3)-based expression of Zika virus antigens illustrates a rapid method of antibody production against emerging pathogens. *Biochimie* **142**, 179–182 (2017).
73. Niu, X. et al. Convalescent patient-derived monoclonal antibodies targeting different epitopes of E protein confer protection against Zika virus in a neonatal mouse model. *Emerg. Microbes Infect.* **8**, 749–759 (2019).
74. Yi, J. et al. Co-delivery of Cas9 mRNA and guide RNAs edits hepatitis B virus episomal and integration DNA in mouse and tree shrew models. *Antivir. Res.* **215**, 105618 (2023).
75. Johnson, B. W., Russell, B. J. & Lanciotti, R. S. Serotype-specific detection of dengue viruses in a fourplex real-time reverse transcriptase PCR assay. *J. Clin. Microbiol.* **43**, 4977–4983 (2005).
76. Yu, L. et al. Delineating antibody recognition against Zika virus during natural infection. *JCI Insight* **2**, https://doi.org/10.1172/jci.insight.93042 (2017).

Acknowledgements

We thank Rui Mao, Jian Zhang, Zhi Wang and Cuie Li in the Animal Center of GIBH for their assistance in animal experiments. This study was partially supported by National Natural Science Foundation of China (32370998 and 82061138006 to Liqiang Feng), National Key R&D Program of China (2023YFF0724200 to Linping Wu), Natural Science Foundation of Guangdong Province (2023A1515011468 to Liqiang Feng), grants from State Key Laboratory of Respiratory Diseases (SKLRD-Z-202311 to Zhengfeng Li), China Postdoctoral Science Foundation (2023M733511 to Zhengfeng Li), Basic Research Project of Guangzhou Institutes of Biomedicine and Health, Chinese Academy of Sciences (No. GIBHBRP24-03 to Linping Wu).

Author contributions

Xinglong Liu, Zhengfeng Li, and Xiaoxia Li performed the animal experiments, and analyzed the data. Weixuan Wu, Huadong Jiang, Yufen Zheng, and Junjie Zhou were involved in the preparation of circRNA-LNPs. Xianmiao Ye and Junnan Lu were involved in the animal experiments and virological and immunological assays. Wei Wang, Lei Yu, Yiping Li, and Linbing Qu provided reagents (viruses and monoclonal antibodies). Jianhua Wang and Feng Li revised the manuscript. Ling Chen, Linping Wu, and Liqiang Feng conceived the study, interpreted the data, and wrote and revised the manuscript. All authors provided feedbacks on each version of the manuscript.

Competing interests

L.C. serves as chief scientific advisor for Guangzhou nBiomed Ltd. The remaining authors declare no competing interests.

Additional information

Supplementary information The online version contains supplementary material available at https://doi.org/10.1038/s41467-024-53242-0.

Correspondence and requests for materials should be addressed to Ling Chen, Linping Wu or Liqiang Feng.

Peer review information *Nature Communications* thanks Claire Huang, who co-reviewed with Bailey MaloneyIn-Jeong Kim and the other, anonymous, reviewer(s) for their contribution to the peer review of this work. A peer review file is available.